SMHI RMK
Nr 51, May 1986

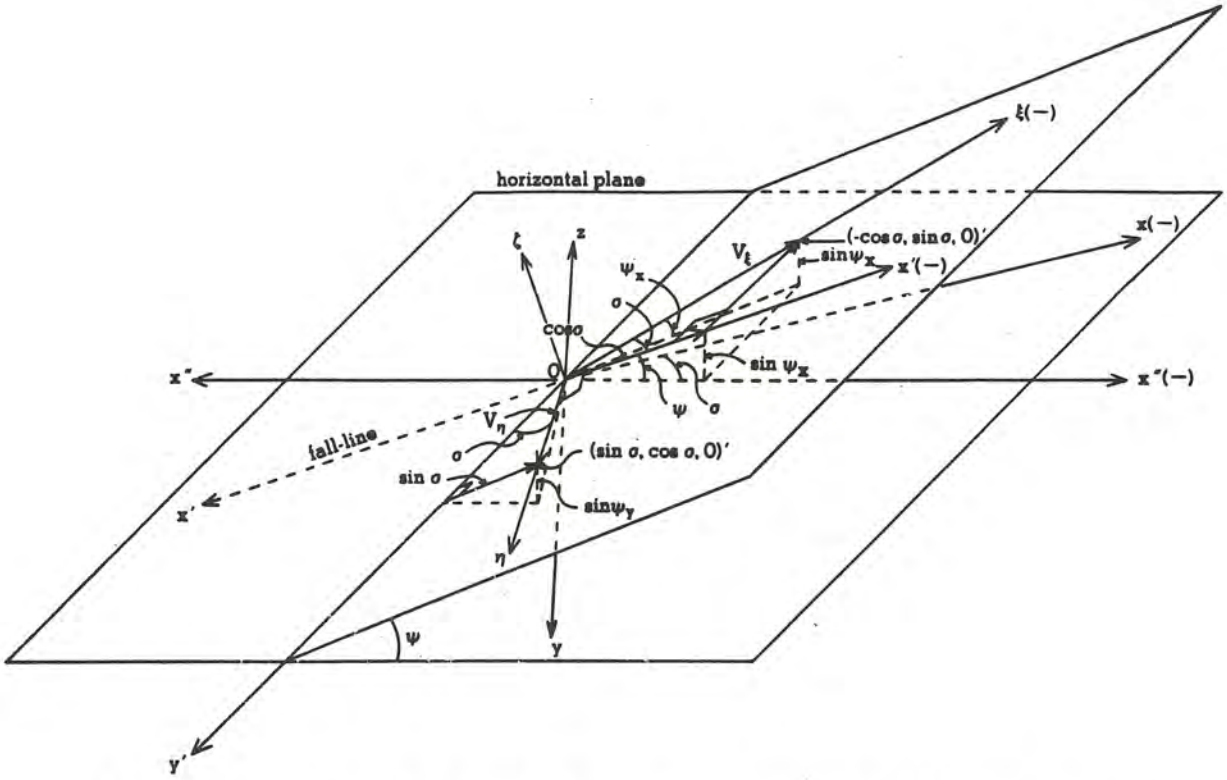

AN ANALYTICAL MODEL OF THE BOUNDARY LAYER ABOVE SLOPING TERRAIN WITH AN APPLICATION TO OBSERVATIONS IN ANTARCTICA

José W. Melgarejo

SMHI REPORTS
METEOROLOGY AND CLIMATOLOGY

Nr 51, May 1986

AN ANALYTICAL MODEL OF THE BOUNDARY LAYER ABOVE SLOPING TERRAIN WITH AN APPLICATION TO OBSERVATIONS IN ANTARCTICA

José W. Melgarejo

SMHIs tryckeri, Norrköping 1986

Issuing Agency
SMHI
S-60176 Norrköping
Sweden

Report number
RMK 51

Report date
May 1986

Author (s)

José W. Melgarejo

Title (and Subtitle)

An Analytical Model of the Boundary Layer Above Sloping Terrain with an Application to observations in Antarctica

Abstract

Analytical solutions of a set of equations that couples the Ekman and the Prandtl boundary layer (BL) equations were obtained; closure on the subgrid scale was via the eddy exchange (K) approach, where K was made to depend on both the internal stability (μ_s) and height raised to an arbitrary power. The boundary layer height (h) was also made to depend on μ_s. As by-products of these solutions, generalized expressions for the universal functions of μ_s, A, B and C and for the resistance and heat-transfer laws (i. e. α, u_*/G and T_*/Θ_o, respectively) for a given set of external parameters (χ, R_o and S) for the general case of the slope angle $0 \leq \psi \leq 10^{-1}$ rad were presented. From this, an interesting and novel result is the finding that there are three different regimes of solutions depending on whether S (or ψ) is less than, equal to or greater than certain critical value S_c (or ψ_c). The solutions for all three regimes were presented in graphical form, from which the appreciable influence of terrain slope on the cross-isobaric inflow angle, the momentum- and heat-transfer is clearly discernible. Also in a preliminary test of the results of this investigation with observations, it is found that the theoretical values of the cross-isobaric angle are in good agreement with the observed values in Antarctica and therefore encouraging for further research.

Key words

universal functions A, B and C
resistance and heat-transfer laws
stability parameter
boundary layer height
sloping terrain
slope angle
slope direction

Supplementary notes

Number of pages
98

Language
English

Excerpts of this report will be published elsewhere.

ISSN and title

0347-2116 SMHI Reports Meteorology and Climatology

Report available from:
The author

CONTENTS

EXTENDED ABSTRACT vii

1. INTRODUCTION 1

2. THE MODEL 2

2.1 Governing equations 2

2.2 Solutions 5

3. EXPRESSIONS FOR THE RESISTANCE LAWS 12

3.1 Sloping surface special case I ($\gamma=0$) 15

3.2 Sloping surface special case II ($G=0$, $\psi<<f/N$) 17

3.3 Sloping surface special case III ($\mu_s= \pm\infty$, $\psi<<f/N$ or $\gamma=0$) 18

4.EXPRESSIONS FOR THE UNIVERSAL FUNCTIONS A, B AND C 21

4.1 Expressions for the height of the boundary layer 21

4.2 Universal functions A and B 22

4.3 The Universal function C 25

4.4 A new model for temperature and the universal function C 26

4.5 Universal constants A, B and C for the neutral case ($\mu_s=0$) 29

4.6 'Smoothed' universal functions A, B and C 31

5. RESULTS 34

5.1 Computation of δ *for* $\mu_s= \pm\infty$ ($\psi<<f/N$ or $\gamma=0$) 34

5.2 Computation of α *for* $\mu_s= \pm\infty$ ($\psi=0$) 35

5.3 Computation of the resistance and heat-transfer laws in the general case (γ and $G \neq 0$, $\psi<\simeq 0.1$ and all χ) 36

6. COMPARISON WITH OBSERVATIONS 40

7. CONCLUSIONS AND FUTURE OUTLOOK 45

8. AKNOWLEDGEMENTS 50

9. APPENDIX A (List of Symbols) 51

10. ABBREVIATIONS 53

11. APPENDIX B (Derivation of the Main Equations) 54

12. APPENDIX C 68

13. APPENDIX D 70

14. REFERENCES 72

15. TABLE I (Universal Constants A, B and C) 76

16. TABLE II 77

17. TABLE III 78

18. FIGURES 79

EXTENDED ABSTRACT

Analytical solutions of a set of equations that couples the Ekman boundary layer (BL) and the Prandtl slope wind equations were obtained. To model the turbulent fluxes due to the subgrid scale phenomena, eddy viscosity and diffusivity coefficients were made to depend on both stability and height raised to an arbitrary power, and the boundary layer height (h) on the internal stability (μ_s). As by-products of these solutions and the boundary conditions, analytical expressions for the universal functions of stability, A, B and C and for the resistance and heat-transfer laws of the Rossby-number similarity theory for the boundary layer above sloping terrain are presented. Laikhtman and Kurdova's (1978) suggestion for the heat-flux distribution in the boundary layer was generalized to include h as an additional parameter. From this, a still more general function C is derived. It is seen that these new stability functions are an improvement of those found by previous investigators.

As to the solutions of the resistance and heat-transfer laws for a given set of external parameters, first three special solutions, two of which have much relevance in Antarctic meteorology, were discussed: For the special case of slope angle (ψ) much less than an order of 10^{-2} rad and in the absence of large scale flow, *explicit* solutions for the surface drag and heat-transfer (T_*/θ_o) coefficients and the direction (δ) of the surface wind from the fall-line vector are obtained. Also for the special case of very large μ_s and $\psi << 10^{-2}$ rad, *explicit* expressions for δ (when $\psi \neq 0$) and for the cross-isobaric inflow angle (α) in the special case of horizontal underlying surface ($\psi = 0$) are derived and found to depend on μ_s

alone. Next, solutions for μ_s, the geostrophic drag (u_*/G) coefficient, T_*/θ_o and α (or δ) for the general case of $0 \leq \psi \leq 10^{-1}$ rad, for all possible directions (χ) of the geostrophic wind ($\underline{G}$) with respect to the fall-line vector and for all values of the external stability (S) and surface Rossby-number (R_o) are obtained. From this, an interesting and novel result is the finding that there are three different types of solutions depending on whether S (or ψ) is less than, equal to or greater than a certain critical value S_c (or ψ_c). It is found that the solution of α for $S < S_c$ is of the 'oscillatory' type, for $S > S_c$ of the 'staircase' type and for $S = S_c$ of the 'transition' type. A physical picture for this behavior of the surface wind with respect to $\underline{G}$ is offered and solutions of α (or δ) μ_s, u_*/G and T_*/θ_o for all three types are presented in graphical form, from which the appreciable influence of terrain slope on the transfers of momentum and heat in the BL (ascompared to the transfers for the case when $\psi = 0$) is clearly discernible.

Also, in a preliminary test of the results of this investigation with observations, it is found that the theoretical values of α (as a function of χ) are in very good agreement with the observed values of α in Antarctica and therefore encouraging for further research.

1. INTRODUCTION

The interplay between thermally active sloping surfaces (i.e. with a definite excess or deficit of heat over that of the overlying air) and the wind and temperature regimes in the boundary layer (BL) has been the topic of theoretical and experimental research for a long time. For example, the so-called katabatic winds (caused by cold and wide sloping surfaces and modified by the action of the Coriolis force) are said to play the role in maintaining the continental ice caps in the interior of Antarctica and Greenland. This interplay is well documented by observations and therefore needs no reiteration. (Lettau and Schwerdtfeger, 1967; Schwerdtfeger, 1972). However, the development of a unified theoretical framework to explain the observational findings has not been so succesful. Recently Gutman and Melgarejo (1981, here-to-forth referred to as GM) proposed such a theoretical model for the BL above sloping terrain in a way that generalizes the formulation of the previous investigators (e.g. Prandtl, 1942; Ball, 1960, Gutman and Malbakhov, 1964). In GM generalized expressions for the resistance and heat transfer laws and the universal functions of stability A, B and C of the Rossby-number similarity theory for the BL above sloping terrain are already given. However, on the influences of terrain slope on the momentum and heat transfers for slope angles even of an order as small as 10^{-3} rad[4], only a qualitative picture was given except for the special case of momentum and heat transfers in the absence of large scale flow and slope angles of order 10^{-1} rad.

---

[4] For abbreviations see Appendix A.

In this paper a thorough revision of the theoretical model in GM is presented. That is, wherever possible the shortcomings of that model are removed and some of the assumptions are generalized so as to make the present theoretical model as general as possible and yet tractable to analytical methods of solution. Then quantitative assessment of the appreciable influence of terrain slope on the momentum and heat transfers is presented in the general case of slope angles varying in the ranges from zero to about an order of 10^{-1} rad (or 10 deg) and for all orientations of the large scale flow (or geostrophic wind) with respect to the fall-line vector (FLV, directed downwards along the direction of greatest slope) and all combinations of the external parameters.

The mathematical model and solutions will be given in section 2, the expressions for the resistance and heat transfer laws in section 3, the expressions for the universal functions, A, B and C in section 4, the results and discussions in section 5, a comparison with observations in section 6 and the conclusions and future outlook in section 7.

2. THE MODEL

2.1. *Governing equations*

In GM, from a balance of Coriolis, frictional and "drainage" (component of the buoyancy force parallel to the FLV) forces in a non-accelerating steady flow, a system of equations for the BL above sloping terrain is derived in a way that conveniently couples the usual Ekman BL equations with the Prandtl slope wind equations. Since

it has been pointed out that the derivation of these equations may be unfamiliar and also for completeness, the following non-dimensional form is derived in detail in Appendix[5] B:

$$\frac{d}{dz}(K \frac{dp}{dz}) - i\, p = 0 \qquad (2.1)$$

$$\frac{d}{dz}(K \frac{dq}{dz}) = 0 \qquad (2.2)$$

To close this system the eddy viscosity K will be modelled quite generally as

$$K = \beta\, z^{\alpha} \qquad (2.3)$$

where α and β can be any non-dimensional functions. The only requirement is that they be independent of z. For reasons that will become apparent later, the form of K in (2.3) is modified without loss of generality to

$$K = \nu^{1-\alpha}\, z^{\alpha} \qquad (2.4)$$

where ν like β can be any non-dimensional function independent of z.

As in GM, the no-slip condition, the condition of finite heating or cooling and the definition for the fluxes at $z=z_o$, and the assumption of vanishing fields at z=h give the following lower and upper boundary conditions for the system (2.1) and (2.2), respectively

---

[5] For notations see the list of symbols in Appendix A.

$$\text{at } z = z_o \begin{cases} p = -a\, n \sin\chi - b\, m + i\, b\, n \cos\chi \\ q = -n \sin\chi + \left(\frac{a}{1-a^2}\right) b\, m \\ z\frac{dp}{dz} = a \sin\delta - b\, \eta/\alpha_H^o - i\, b \cos\delta \\ z\frac{dq}{dz} = \sin\delta + \left(\frac{a}{1-a^2}\right) b\, \eta/\alpha_H^o \end{cases} \tag{2.5}$$

and

$$\text{at } z = h, \quad p = q = 0 \tag{2.6}$$

The boundary conditions (2.5) arise from the physical requirement of no motion and therefore large vertical gradients at the surface and (2.6) from the requirement that the deviation fields from a background atmosphere (see Appendix B) vanish at the top of the BL.

Finally, the conjugate conditions (at $z = \nu$) imposed to achieve continuous solutions are:

$$\text{at } z = \nu \begin{cases} p|_{z=\nu+0} = p|_{z=\nu-0} \; ; \; \frac{dp}{dz}|_{z=\nu+0} = \frac{dp}{dz}|_{z=\nu-0} \\ q|_{z=\nu+0} = q|_{z=\nu-0} \; ; \; \frac{dq}{dz}|_{z=\nu+0} = \frac{dq}{dz}|_{z=\nu-0} \end{cases} \tag{2.7}$$

The other definitions in (2.5) have the following meaning:

$$n = kG/u_*, \qquad \eta = \mu_s \psi/k^2, \qquad m = n\, \theta_o/T_* \tag{2.8}$$

and the sense of the angles δ, ψ and χ is given in Fig. 2.

This completes the formulation of the problem. The solutions will be given next.

2.2. *Solutions*

Since the solutions of (2.1) and (2.2) determine totally the shape of the universal functions A, B and C as will be seen later, much effort was devoted to finding as complete and as general solutions as possible for the model of K in (2.4) and the boundary conditions (2.5) and (2.6), such that any further improvements of the solutions would have to be made by revising the model of K and/or by introducing a more general formulation of the problem.

As to the solution for p, it is interesting to note that the form of (2.1) for the model of K in (2.4) is a special form of the following more general differential equation with variable coefficients, called here "transformed Bessel's modified differential equation",

$$\frac{d}{dz}\left(\nu^{1-\alpha} \cdot z^{\alpha} \frac{dp}{dz}\right) - i\, z^{\alpha-2}\,(z^{\gamma} + \delta)\, p = 0 \qquad (2.9)$$

where α, ν, γ, and δ are all arbitrary constants. Observe that the transformations

$$\begin{aligned} p &= z^{(1-\alpha)/2}\, \tilde{p}\,(\xi) \\ \xi &= 2(i\, \nu^{\alpha-1} \cdot z^{\gamma})^{1/2}/\gamma \end{aligned} \qquad (2.10)$$

will reduce (2.9) to the more familiar "Bessel's modified differential equation of order n",

$$\xi^2 \frac{d^2\tilde{p}}{dz^2} + \xi \frac{d\tilde{p}}{dz} - (\xi^2 + n^2)\tilde{p} = 0 \qquad (2.11)$$

where

$$n = [(\alpha-1)^2 + i\ 4\ \nu^{\alpha-1}\delta]^{1/2}/\gamma \tag{2.12}$$

From (2.11) it follows in the usual notation for Bessel functions that the general solution of (2.9) is

$$p = z^{(1-\alpha)/2} \cdot \begin{cases} a\ I_n(\xi) + b\ I_{-n}(\xi), & n \neq \text{integer} \\ a\ I_n(\xi) + b\ K_n(\xi), & \text{all } n \end{cases} \tag{2.13}$$

where

$$\xi = 2\ (i\ \nu^{\alpha-1} \cdot z^{\gamma})^{1/2}/\gamma \tag{2.14}$$

and I_n and K_n are respectively the modified Bessel functions of the first and second kind and of order n. In this investigation n is defined in (2.12) and a and b are arbitrary constants. The definitions of I_n and K_n can be found in standard text books on Bessel functions (e.g. Watson, 1944).

From (2.9) and (2.13), it is a simple step to extract the solution of (2.1) which corresponds to K in (2.4). Thus by simply setting $\delta = 0$ and $\gamma = 2 - \alpha$ in (2.9), (2.12) and (2.14), the general solution of (2.1) for K in (2.4), irrespective of the sign of n in (2.12), is (2.13) for n and ξ given by

$$\begin{aligned} n &= (\alpha-1)/(2 - \alpha) \\ \xi &= \xi_\alpha = 2\ (i\nu^{\alpha-1}z^{2-\alpha})^{1/2}/(2 - \alpha) \end{aligned} \tag{2.15}$$

The model of K in (2.4) is a generalization of the previous

models of K that have appeared in the literature. It includes α as an independent parameter, such that the particular solutions of (2.1) or (2.2) for the particular model of K can be recovered simply by choosing the corresponding values of α; e.g., the well-known solutions for constant K can be recovered by setting $\alpha = 0$ in (2.4), etc. The model in GM corresponds to $\alpha = (2 \pm 2)/3$ in (2.4) for the unstable and stable cases respectively when $\nu \leqslant z \leqslant h$ and it corresponds to $\alpha = 1$ when $z_o \leqslant z \leqslant \nu$. That is

$$K = \begin{cases} z & , \quad \alpha = 1 \ , \text{ all } \mu_s, \quad z_o \leqslant z \leqslant \nu \\ (z^4/\nu)^{1/3}, & \alpha = 4/3, \ \mu_s < 0 \quad \nu \leqslant z \leqslant h \\ \nu & , \quad \alpha = 0 \ , \ \mu_s > 0 \end{cases} \tag{2.16}$$

where

$$\nu = \begin{cases} \zeta_u/\mu_s & , \quad \mu_s < 0 \\ 1/(\beta_u \mu_s), & \mu_s > 0 \end{cases} \tag{2.17}$$

$$\mu_s = \lambda_s/L = a\,\mu \qquad [\ L = u_*^2/(k^2 \beta T_*)\ ] \tag{2.18}$$

and ζ_u and β_u are constant coefficients whose physical meaning will be given later. Other examples of solutions of (2.1) for a particular model of K obtained by a particular choice of α in (2.4) can be found in Zilitinkevich et al. (1967).

In what follows, this investigation will be concerned only with the generalized solutions (2.13) that correspond to the special model of K in (2.16). First, the solutions for $\alpha = (2 \pm 2)/3$ from (2.13) - (2.15) are

$$p = z^{\frac{-1}{2 \pm 4}} \left[a\, I_{1/2}(\xi_z) + b\, I_{-1/2}(\xi_z) \right] \tag{2.19}$$

which, with the following expressions for the Bessel functions $I_{1/2}$ and $I_{-1/2}$,

$$I_{1/2}(x) = \left(\frac{2}{\pi x}\right)^{1/2} \sinh x$$

$$I_{-1/2}(x) = \left(\frac{2}{\pi x}\right)^{1/2} \cosh x \tag{2.20}$$

and the boundary conditions (2.6), can be more elegantly written as

$$p = C_3 z^{-(1\pm1)/6} \sinh(\xi_z - \xi_h) \tag{2.21}$$

where

$$\xi_z = (2 \pm 1)[i\nu^{1/(1\pm2)}]^{1/2} z^{1/(2\pm1)} \tag{2.22}$$

and ξ_h is obtained from (2.22) by setting $z = h$. C_3 is an arbitrary constant. In (2.21) and (2.22) the upper sign is for the case when $K \equiv (z^4/\nu)^{1/3}$ and the lower sign for the case when $K \equiv \nu$.

Next the solution of (2.1) for $K \equiv z$ from (2.13) and (2.15) which corresponds to $\alpha = 1$ and therefore to $n = 0$ from (2.15) is

$$p = a\, I_0(\xi_z) + b\, K_0(\xi_z) \tag{2.23}$$

where

$$\xi_z = 2\,(iz)^{1/2} \tag{2.24}$$

and a and b are arbitrary constants as before. Note that the definitions of α, γ, a, b, and n in this sub-section are not to be confused with the definitions of the same elsewhere.

As to the solution for q, the solution of (2.2) for the model of K in (2.16) is straightforward and will be given below without further discussion.

In summary, the solutions for p and q from (2.1) and (2.2) which conform with the model of K in (2.16) and written in a more familiar notation are respectively:

$$p = \begin{cases} (C_1 + C_2 \ln z)\, H(iz) - 2C_2\, M(iz), & \text{all } \mu_s,\ z_o \leq z \leq \nu \\ C_4 \sinh\left[(i/\nu)^{1/2}\,(z-h)\right], & \mu_s > 0 \\ C_3\, z^{-1/3} \sinh\left[3i^{1/2}\nu^{1/6}(z^{1/3} - h^{1/3})\right], & \mu_s < 0 \end{cases} \quad \nu \leq z \leq h \qquad (2.25)$$

$$q = \begin{cases} c_1 + c_2 \ln z, & \text{all } \mu_s,\ z_o \leq z \leq \nu \\ c_4\,(z-h), & \mu_s > 0 \\ c_3\,(z^{-1/3} - h^{-1/3}), & \mu_s < 0 \end{cases} \quad \nu \leq z \leq h \qquad (2.26)$$

where

$$H(iz) = \sum_{n=0}^{\infty} (iz)^n/(n!)^2$$

$$M(iz) = \sum_{n=0}^{\infty} \Phi_n \cdot (iz)^n/(n!)^2 \qquad (2.27)$$

$$\Phi_n = \sum_{\kappa=1}^{n} 1/\kappa, \qquad \Phi_o = 0$$

and C_1, C_2, C_3, C_4 and c_1, c_2, c_3, c_4 are arbitrary complex and real constants of integration respectively.

It can be seen that (2.25) - (2.27) are a generalization of the

solutions in GM not only to include the height h of the BL as an additional parameter but also to include all powers of z in the first expression for p, which can be necessary when ν is not so small near neutral cases. The solutions in GM can be recovered by letting $h \to \infty$ in (2.25) and (2.26) and neglecting in (2.27) all terms with powers of z higher than one.

In retrospect, it is seen that the first expression for p in (2.25) can also be obtained by substituting into (2.1) a power series of the form

$$p = \sum_{n=0}^{\infty} a_n z^n + \ell n\, z \sum_{n=0}^{\infty} b_n z^n \tag{2.28}$$

and solving for the coefficients a_n and b_n to obtain

$$\begin{aligned} a_n &= (a_o - 2\phi_n b_o)\, i^n/(n!)^2, \qquad n \geq 0 \\ b_n &= b_o\, i^n/(n!)^2 \qquad\qquad , \qquad n \geq 0 \end{aligned} \tag{2.29}$$

Along the same theoretical lines of this latter approach, the solution of (2.1) for K in (2.16) and for the special case of $z \ll 1$ has already been presented e.g. in Kazanski and Monin (1961), Laikhtman and Yordanov (1978) and in GM. It is easy to see that by substituting (2.29) into (2.28) the first expression for p in (2.25) and the definitions (2.27) will be recovered.

As to the physical meaning of the constant coefficients β_u and ζ_u in (2.17), it can be shown that β_u is the inverse of the critical Richardson flux number $R_{i,fc}$, (Businger et al., 1971)

$$R_{i,f} = \zeta/\phi(\zeta) = \zeta/(1 + \beta_u \zeta) \tag{2.30}$$

where $\zeta = z/L$ is a non-dimensional height, $\phi(\zeta)$ some universal function and L the Monin-Obukhov length scale defined in (2.18). From (2.30) it is seen that

$$\lim_{\zeta \to +\infty} R_{i,f} \equiv R_{i,fc} = 1/\beta_u \qquad (2.31)$$

The value of β_u according to recent investigations regarding $R_{i,fc}$ (e.g. in Louis et al., 1981 and Laikhtman and Kurdova, 1980) is close to eight, i.e. for $R_{i,fc} = 0.125$.

On the other hand, ζ_u is related to the value of ζ, say $\zeta = \zeta'$, at which transition from unstable to free-convection regime in the surface layer takes place. Also from recent investigations, e.g. in Kazakov and Lazriev (1978), regarding the shapes of eddy viscosity and eddy exchange coefficients in free-convection in the surface layer, the following expression for ζ_u can be derived

$$\zeta_u = \zeta/(1 - 15\,\zeta)^{3/4} \qquad \text{at } \zeta = \zeta' \qquad (2.32)$$

The value of ζ' from Kazukov and Lazriev is -8.21. It is seen that for $\zeta' = -8.21$ in (2.32), $\zeta_u = -0.22$ is obtained, which is about three times greater than the more conventional value of $\zeta_u = -0.07$ used in GM and in many other investigations. Test calculations carried out for both values of ζ_u showed that better results are obtained for the choice of $\zeta_u = -0.22$.

In the next section the solutions (2.25) - (2.27) will be utilized to derive expressions for the resistance and heat-transfer laws of the Rossby-number similarity theory for the BL above sloping terrain.

3. EXPRESSIONS FOR THE RESISTANCE AND HEAT-TRANSFER LAWS

As discussed in GM, care must be taken in introducing the definitions of the real functions A, B and C into the derivation of the resistance and heat transfer laws based on the solutions (2.25) - (2.28). Non-judicious methods of definition will result in making these functions dependent not only on the internal stability parameter μ_s but also on the other parameters such as α (or δ), thus making them more difficult to determine at least from observations. It is shown in GM that the following definitions

$$\frac{C}{C_2}_1 = B + i\,A + \ell n\, k \qquad \text{and} \qquad \frac{c}{c_2}_1 = C + \ell n\, k \tag{3.1}$$

have the desirable feature of making these functions depend on μ_s alone.

This means that by changing the slope angle ψ (even for the choice of $\psi = 0$) only the argument of these functions will be changed but not their shape. From this the interesting conclusion is that the A, B and C functions so derived are the very same universal functions derived when solving the problem of the BL above a horizontal surface and which are currently the topic of much theoretical and observational research. The other definitions e.g. those that are introduced in Laikhtman and Yordanov (1979) do not give this desirable property.

The above conclusion will make it possible to compare and exchange the A, B and C functions thus found in this investigation with those in other investigations. Then following the method in GM, because of the smallness of $z_o << 1$, first the solution (2.25) for

$z = z_o$ is reduced with a high degree of approximation to

$$\left.\begin{aligned} p &= C_1 + C_2 \ln z; & q &= c_1 + c_2 \ln z \\ z\frac{dp}{dz} &= C_2; & z\frac{dq}{dz} &= c_2 \end{aligned}\right\} \text{at } z = z_o \qquad (3.2)$$

Next, substituting (3.2) into the lower boundary conditions (2.5) and combining the result with (3.1), gives the following generalized expressions for the resistance and heat transfer laws for the BL above sloping terrain

$$\begin{aligned} -a\, n\, b \sin\chi - m &= (B + \ell)(a\, b \sin\delta - \eta/\alpha_H^o) + A\cos\delta \\ n\cos\chi &= -(B + \ell)\cos\delta + A(a\, b \sin\delta - \eta/\alpha_H^o) \\ -n\, b \sin\chi + \frac{a}{1-a^2} m &= (C + \ell)(b \sin\delta + \frac{a}{1-a^2}\eta/\alpha_H^o) \end{aligned} \qquad (3.3)$$

where[6] n, m and η are as defined in (2.8),

$$\begin{aligned} \ell &= \ln(k\bar{z}_o) = \ln\left(\frac{n}{k\, a\, R_o}\right) \\ R_o &= \frac{G}{fz_o} \qquad (b = \text{sign}\,\phi) \end{aligned} \qquad (3.4)$$

and A, B and C are the universal functions of μ_s alone. The parameter b is introduced to make (3.3) applicable for either Northern or Southern Hemispheres.

Upon substituting from (3.3) into the following definition of the external stratification parameter S,

---

[6] The overbar in z_o is kept to avoid ambiguity.

$$S = - \beta \theta_o/(f G) \tag{3.5}$$

the following implicit relationship for the computation of μ (or equivalently of $\mu_s = a \mu$) in terms of S is obtained:

$$\mu = -k^2 \alpha_H^o \frac{n S - [(1 - a^2)/(a\psi)][(B-C)a b \sin \delta + A \cos \delta]}{C + \ell + (1 - a^2)(B - C)} \tag{3.6}$$

The transcendental system of equations (3.3) - (3.6) is now closed in the sense that there are four equations for the four unknowns n, m, δ (or α) and μ (or μ_s) and can be solved for a given set of the non-dimensional external parameters S and R_o and the dimensional external parameters N and f and the angles χ and ψ.

From (3.3) it is not difficult to see that there are various special cases of interest for the resistance and heat transfer laws which can be extracted for a special set of the external parameters. For example, in GM two special cases of interest were discussed in some detail. In the present study, three other special cases of much interest in certain meteorological applications will be dealt with in subsections a,b and c. As will be seen, for purposes of obtaining either the general or special solutions, it is expedient to transform the system (3.3) - (3.6) to the following more convenient form

$$\begin{aligned} -n \cos \alpha &= (B + \ell) - b_1 \\ -b\, n \sin \alpha &= a A - b_2 \\ m &= \eta (C + \ell + b_5) \end{aligned} \tag{3.7}$$

and

$$\mu = -k^2\alpha_H^o \frac{n\,S - a\,\psi(N/f)^2[(B-C)a\,b\sin\delta + A\cos\delta]}{C + \ell + (a\,\psi\,N/f)^2(B - C)} \qquad (3.8)$$

where

$$\begin{aligned} b_1 &= (B - C)[a\tilde{\eta} + (1 - a^2)b\sin\delta]b\sin\delta - A\,\tilde{\eta}\cos\delta \\ b_2 &= (B - C)[a\tilde{\eta} + (1 - a^2)b\sin\delta]\cos\delta + A\,\tilde{\eta}\,b\sin\delta \\ b_5 &= [(B - C)(\tilde{\eta} - a\,b\sin\delta) - A\cos\delta]\left(\frac{k\,N}{f}\right)^2 \alpha_H^o \frac{a\,\psi}{\mu} \\ \tilde{\eta} &= \eta/\alpha_H^o \end{aligned} \qquad (3.9)$$

and the notation b_5 is used to conform with the notation in GM. Also from (B27), it is seen that $(1 - a^2) = (a\,\psi\,N/f)^2$.

3.1. *Sloping Surface Special Case* I ($\gamma = 0$)

In the atmosphere this case corresponds commonly to the stable BL capped by a well-mixed potential-temperature layer, where $\gamma \simeq 0$ even in the prescense of large-scale flow. This situation can arise particularly in low and middle latitudes over land in the summer when the BL in its diurnal cycle switches from a deep, well-mixed daytime unstable layer to a much less mixed and shallow nighttime stable layer. This case has been studied e.g. by Brost and Wyngaard (1978).

Thus $\gamma = 0$ (or $N = 0$) in (B27) gives $a = 1$. By substituting $a = 1$ and $N = 0$ into (3.7) - (3.9) and then solving for n, α, m and μ, the following simpler relations for the resistance and heat transfer laws and μ are arrived at:

$$(B + \ell)^2 + A^2 = b_3^2 + b_4^2 \qquad (B + \ell \leq 0) \qquad (3.10)$$

$$\sin\alpha = -b\,[A\,b_3 + b_4(B + \ell)]/(b_3^2 + b^2{}_4)$$

$$\cos\alpha = [A\,b_4 - b_3(B + \ell)]/(b_3{}^2 \neq \beta_4{}^2) \tag{3.11}$$

$$\theta_0/T_* = (C + \ell)/\alpha_H^0 \tag{3.12}$$

and

$$\mu = -k^2\,\alpha_H^0\,\frac{n\,S}{C + \ell} \tag{3.13}$$

where

$$\begin{aligned} b_3 &= Q\cos z + n \\ b_4 &= b\,Q\sin z \\ Q &= |\tilde{n}|\,[A^2 + (B - C)^2]^{1/2} \\ z &= \chi + b\arg[A\tilde{n},\,(B - C)\tilde{n}] \quad (\tilde{n} = n/\alpha_H^0) \end{aligned} \tag{3.14}$$

and ℓ is defined in (3.4). Here arg stands for the argument of the complex number, say, $f = x + i\,y$, whose definition can be written as

$$\arg(x,y) = \tan^{-1}(y/x) + [1 - \mathrm{sign}(x)]\,\mathrm{sign}(y)(\pi/2) \tag{3.15}$$

Note that (3.15) in terms of the FORTRAN standard function ATAN2 is arg (x,y) = ATAN2 (y,x).

It can be seen that by setting $\psi = 0$ into (3.10), (3.11) and (3.14), the corresponding expressions for the BL above a horizontal surface can be recovered.

3.2. *Sloping Surface Special Case II* ($G = 0$, $\psi \ll f/N$)

The atmospheric counterpart of this case has been observed to occur approximately during the winter months in the ice-caps of Antarctica and Greenland at the time when the surface cooling by radiation is intense. For example, in Gutman and Malbakhov (1964) a non-stationary model of the BL was developed to study this situation (which corresponds to "katabatic winds" in the usual terminology) in the interior of Antarctica in the absence of geostrophic wind ($G = 0$) but under the influence of Coriolis forces ($f \neq 0$). Their results seem to have compared favorably with observations.

Thus, by setting $\psi \ll f/N$ in (B27), $a \simeq 1$ is obtained. Since $G = 0$ and $a = 1$, $n = 0$ and $\ell = \ell n(fz_o/u_*)$ are obtained from (2.11) and (3.4) respectively. Furthermore, since the system (3.3) is independent of χ, χ can be defined at will and α will be obtained from $\chi = \alpha + \delta$. Thus $\chi = 0$ gives $\alpha = -\delta$. By substituting $n = 0$ and $a = 1$ into (3.7) - (3.9), the following expressions for $\tilde{U}/u_*$, δ, θ_o/T_* and μ are obtained:

$$B + \tilde{\ell} = - A\, T - 2\, \ell n(f/N) \quad [\tilde{\ell} = \ell n(\tilde{U}/u_*)] \tag{3.16}$$

$$\sin \delta = b\, \mathfrak{N}\, (1 - I\, T) \,/\, (1 + T^2)$$

$$\cos \delta = \mathfrak{N}\, (I + T) \,/\, (1 + T^2) \tag{3.17}$$

$$\alpha_H^o \frac{\theta_o}{T_*} = - A\, (I + T) + b_5 \tag{3.18}$$

and

$$\mu = -k^2 \alpha_H^o \frac{\tilde{n}\,\tilde{S} - \psi(N/f)^2\,[(B - C)b \sin\delta + A\cos\delta]}{C + \tilde{\ell} + (\psi\, N/f)^2\,(B - C) + 2\,\ell n\,(f/N)} \tag{3.19}$$

where

$$I = (B - C)/A$$

$$T = \text{sign}\,(A)\,[\tilde{\eta}^2(1 + I^2) - 1]^{1/2} \tag{3.20}$$

$$b_S = [(B - C)(\tilde{\eta} - b\sin\delta) - A\cos\delta]\,(\frac{k\,N}{f})^2\,\frac{\psi}{\mu}\,\alpha_H^o$$

$$\tilde{n} = k\,\tilde{U}/u_* \quad , \qquad \tilde{U} = z_o N^2/f$$

$$\tilde{S} = -\alpha_H^o\,\theta_o/(\gamma z_o)$$

Note that (3.16) and (3.17) are also special cases of (3.10) and (3.11). This can be seen by setting $n = 0$ and $\chi = 0$ in (3.14) and substituting $\alpha = -\delta$ into (3.11).

Furthermore from (3.17) it follows that

$$\delta = b\,\arg\,[\tilde{\eta}\,(I + T),\ \tilde{\eta}(1 - I\,T)] \tag{3.21}$$

For μ known, (3.16), (3.18) and (3.21) are the *explicit* solutions for $\tilde{U}/u_*$, θ_o/T_* and δ respectively. However, when μ is not known a priori, the relations (3.16) - (3.19) become implicit in μ and the solutions for $\tilde{U}/u_*$, θ_o/T_* and δ are more difficult to find.

3.3. *Sloping Surface Special Case III* ($\mu_s = \pm\infty$, $\psi \ll f/N$ or $\gamma = 0$)

As seen in subsections a and b, the effect of the simplifying

assumptions $\psi \ll f/N$ and $\gamma = 0$ is to give first $a = 1$ and then to reduce the system (3.7) - (3.9) to the simplified system (3.10), (3.11) and (3.14) for n and α. From this system and under quite general assumptions regarding the functions A, B and C, the following interesting expressions for the direction δ of the surface wind (from the FLV when $\psi \neq 0$) or for the cross-isobaric inflow angle α (when $\psi = 0$) in the limit of $\mu_s = \pm\infty$ are obtained:

(a) In the case of $\psi \neq 0$, the further assumptions of $Q \to \infty$ in (3.14) and $B/Q \to 0$ as $\mu_s \to \pm\infty$ (which are probably true for all A, B and C functions used in practical applications) yield

$$\lim_{\mu_s \to \pm\infty} \delta = -b \lim_{\mu_s \to \pm\infty} \arg [A \hat{\eta}, (B-C)\hat{\eta}] \qquad (\psi \neq 0) \qquad (3.22)$$

(b) In the case of $\psi = 0$ and therefore $a = 1$ and $\eta = 0$ exactly, the system (3.10) and (3.11) is reduced to

$$\begin{aligned} & A^2 + (B + \ell)^2 = n^2 \qquad (B + \ell \leq 0) \\ & n = k R_o e^{\ell} \\ & \sin \alpha = -bA/n \\ & \cos \alpha = -(B + \ell)/n \end{aligned} \qquad (3.23)$$

Next, for any particular value μ_o of μ_s, it is seen that (3.23) has a real solution if and only if

$$|A| \leq k R_o e^{-B} \qquad \text{at } \mu_s = \mu_o \qquad (3.24)$$

If this condition (3.24) is satisfied in a neighborhood of $\mu_s = \mu_o$ (including $\mu_o = \pm\infty$), then the following asymptotic formulae

hold:

$$n \sim \begin{cases} \text{solution of (3.23)}, & \text{if } B \to \text{finite value} \\ (A^2 + B^2)^{1/2}, & \text{if } B \to -\infty \\ k\, R_o\, e^{-B}, & \text{if } B \to +\infty \end{cases} \tag{3.25}$$

$$\lim_{\mu_s \to \mu_o} \alpha = \begin{cases} \text{solution of (3.23)}, & \text{if } B \to \text{finite value} \\ b \tan^{-1}\left[\lim_{\mu \to \mu_o} (A/B)\right], & \text{if } B \to -\infty \\ -b \tan^{-1} \lim_{\mu_s \to \mu_o} \dfrac{\text{sign}(A)}{[(k\, R_o\, e^{-B}/A)^2 - 1]^{1/2}} & \text{if } B \to +\infty \end{cases} \tag{3.26}$$

It is interesting to note that although ultimately the value of δ should depend only on the stability parameter μ_s, here it depends, as seen from (3.22), (3.25) and (3.26), also on the values of the functions A, B and C or A and B for the case when $\psi \neq 0$ or $\psi = 0$ respectively. That lim δ when $\psi \neq 0$ should depend not only on A and B but also on C is consistent with the model equations (B20), where momentum and temperature fields are coupled by the very terms which contain ψ. On the other hand, when $\psi = 0$ this is no longer the case.

More detailed theoretical investigations and comparisons with observations of the results in subsections 3a, 3b and 3c could well be the topic of a separate paper. As stated earlier, the aim in the present study is to obtain the solutions of (3.7) - (3.9) for the general case of $a \neq 1$, $G \neq 0$, $f \neq 0$, for ψ varying in the range of $0 \leq \psi \leq 10^{-1}$rad and for all possible values of χ, but first the expressions for the universal functions A, B and C will be derived.

4. EXPRESSIONS FOR THE UNIVERSAL FUNCTIONS A, B and C

In the context of the theory in GM, the precise knowledge of the A, B and C functions has proven to be necessary to obtain sensible results for the resistance and heat transfer laws from the system (3.3) - (3.6) or equivalently (3.7) - (3.9). At the beginning of this investigation, the A, B and C functions of Arya (1975), reputed to be the best available functions derived from observations, were utilized in solving the system (3.7) - (3.9). However, experimentation soon showed that in many cases these A, B and C yielded quite unreasonable solutions (at least from a theoretical point of view). This circumstance prompted a search for alternative functions. The theoretical functions derived in GM were tested and results showed that the former functions produced results which were closer to the expected results for the same cases where Arya's failed. For these and other reasons, primarily because their validity is for only a limited range of μ_s, Arya's functions were abandoned.

4.1. *Expressions for the height h of the BL*

From the Rossby-number similarity theory postulate, it follows that the height h of the BL must also be a function of the stability μ_s alone. In the spirit of the papers by Zilitinkevich (1972) and Zilitinkevich and Monin (1974), such an equation for h is

$$h \simeq (K_h)^{1/2} \tag{4.1}$$

where h and K_h are non-dimensional variables defined in (B30) and, in

the nomenclature of Charney, K_h is the effective value of the eddy viscosity K, which can be obtained from (2.16) by simply replacing z by h. It was Charney (1969) who first suggested an analogous expression for h for the neutral case, which was later generalized by Zilitinkevich (1972) and Zilitinkevich and Monin (1974) to include the effects of stratification.

Thence substituting from (2.16) and (2.17) into (4.1), the following expression for h is arrived at

$$h = \sigma^{1-\varepsilon/2} \nu^{\varepsilon/2} \tag{4.2}$$

where

$$\varepsilon = \text{sign } (\mu_s) \tag{4.3}$$

and σ is assumed to be a constant whose numerical value depends on the stratification.

As to the numerical values of σ in (4.2), experimentation and data simulation show that $\sigma = 1000$ and $\sigma = 10^{-1}$ for the stable and unstable cases respectively, produce the most sensible results.

4.2. *Universal functions A and B*

In the hopes of deriving as exact an expression as possible for the functions A and B as pointed out earlier, the painstaking task of utilizing the exact solutions (2.25) - (2.28) to derive these functions was undertaken. Except for the limitations imposed by the simple model of K in (2.5), these new functions are exact in the context of the present theory. The derivation of the function C will

be given in the next subsection.

Thus as in GM, the new functions A and B are obtained by substituting the solutions (2.25) - (2.27) into (2.7) and then combining with (3.1). The result in complete form is,

$$A = \sum_{n=-1}^{\infty} a_n x^n$$

$$B = -\ell n\,(k x^2) + \sum_{n=-1}^{\infty} b_n x^n \qquad (4.4)$$

where

$$x = \nu^{1/2}$$

$$a_n = -Re(R_n)\sin(n\pi/4) - Im(R_n)\cos(n\pi/4)$$

$$b_n = Im(R_n)\sin(n\pi/4) - Re(R_n)\cos(n\pi/4) \qquad (4.5)$$

$$R(\Delta) = \sum_{n=-1}^{\infty} R_n \Delta^n$$

Here a_{-1} and b_{-1} are both zero for the unstable case ($\mu_s < 0$), and the notations Re and Im stand respectively for the real and imaginary parts of R_n. The generating function R for R_n is given in Appendix C.

Preliminary experiments were carried out with A and B as defined in (4.4) and (4.5) respectively, for various constant values of h and for h a function of μ_s as defined in subsection c. The results indicated that for the values of h tested and for μ_s as small as $|\mu_s| \simeq 1$, the infinite series can be truncated with good approximation at n = 3 in the stable case and n = 4 in the unstable case.

For purposes of future use and comparison with the expressions of

other investigators, the infinite series (4.4) for powers of x up to 3 for the stable case are

$$\left.\begin{aligned} A &= -f/x - g\,x - (fg/3 - 2/3)x^2 + (f/2)x^3 \\ B &= -\ell n(k\,x^2) + g/x + 1 - fx + (cd/3)x^2 - (g/2)x^3 \end{aligned}\right\} (\mu_s > 0) \qquad (4.6)$$

and for powers of x up to 4 for the unstable case are

$$\left.\begin{aligned} A &= -9\,g\,x - 10x^2 - 9\,fx^3 \\ B &= -\ell n\,(k\,x^2) - 3 - 9\,fx + 9\,gx^3 + (17/4)x^4 \end{aligned}\right\} (\mu_s < 0) \qquad (4.7)$$

where

$$\begin{aligned} x &= \nu^{1/2} \\ f &= (c - d)/2^{1/2} \\ g &= (c + d)/2^{1/2} \\ c &= \sinh(\theta)/[\cosh(\theta) + \varepsilon\cos(\theta)] \\ d &= \varepsilon\sin(\theta)/[\cosh(\theta) + \varepsilon\cos(\theta)] \end{aligned} \qquad (4.8)$$

and

<u>stable</u> ($\mu_s > 0$)	<u>unstable</u> ($\mu_s < 0$)
$\theta = -(2\sigma)^{1/2}$	$\theta = -3(2\sigma)^{1/2}$
$\sigma = 1000$	$\sigma = 10^{-1}$
$\varepsilon = 1$	$\varepsilon = -1$

(4.9)

Note that the missing powers of x in (4.6) and (4.7) all have zero coefficients.

As was said regarding the solutions (2.25) - (2.27), it should also be said here that the new expressions (4.6) and (4.7) for A and B respectively are a generalization of the expressions derived in GM not only to include the height h of the BL as an independent parameter, but also to include powers of x higher than one. In (4.6) and (4.7) upon letting $h \to \infty$ and neglecting powers of x higher than one, the formulas for A and B in GM are recovered exactly. Moreover, the infinite series in (4.4) still seems to be convergent for all $|\mu_s| \geq 1$ and for h either <u>any</u> constant value or a function of μ_s in the form defined in subsection a.

4.3. *The universal function C*

As to the derivation of function C, substituting the corresponding solutions for q in (2.26) into (2.5) first and then combining the result with (3.1) yields

$$C = - \ell n\,(k\nu) + 1 - (h/\nu) \tag{4.10}$$

for the stable case and

$$C = - \ell n\,(k\nu) - 3 + 3(\nu/h)^{1/3} \tag{4.11}$$

for the unstable case.

The expressions (4.10) and (4.11) for C are exact in the sense that no approximations are introduced into the derivation. Although

these functions are exact and give improved results over those of Arya (1975) in the sense that they are valid for greater values of $|\mu_s|$, a closer examination showed that they needed improvement especially in the range of $|\mu_s| \leq 10$. Thus attention was turned to finding ways to improve them.

4.4. *A new model for temperature and the universal function C*

Recently, in Laykhtman and Kurdova (1980) an improved equation for the distribution of heat-flux in the BL was suggested, which is followed-up and generalized to include h as an additional parameter. An interesting feature of this equation is that it has three free parameters two of which are connected with the boundary values H and γ (Appendix A) and the third one allows for curvature in the heat-flux profile. It seems that this equation should be sufficient to satisfactorily describe the distribution of temperature in most situations. From this, an equation for the temperature is derived which in non-dimensional form can be written as[7]

$$\frac{d\theta'}{dz} = \frac{c_2\,(1 - z/h)}{K + r\,z^2} \qquad (\bar{\theta}' = \theta'/T_*) \qquad (4.12)$$

where r is the third free parameter mentioned above, whose numerical value will be determined by experimentation. The other two are absorbed in the definitions of θ' and K. It can be seen from (2.5) and (3.2) the value of c_2 for the case of the BL above a

---

[7] Overbars to indicate non-dimensional variables are omitted for simplicity.

horizontal surface is $c_2 = 1/\alpha_H^o$.

From (4.12) it is seen that for $z = z_o$ and $z = h$, the expressions for the constant heat flux in the surface layer and the heat flux in the free atmosphere are recovered, respectively. For the model of K in (2.4), it is interesting to note that the integral of (4.12) is a particular form of the following more general integral[8]:

$$\theta' = \int \frac{\sum_{k=0}^{M} a_k z^k}{a z^{\alpha} + b z^{\beta}} \, dz \qquad (4.13)$$

whose solution is given in Appendix D.

The particular solutions of θ' corresponding to the model of K in (2.5) are easily obtained from (D2) by simply setting the values of the corresponding parameters. Thus from (D2) the solutions are:

a) For the neutral case, the solution for $K = z$ and $h = 1$ is

$$\theta' = -c_2 \, \ell n \, \{[(1+rz)^{1+1/r}]/z\} + c_1 \qquad (4.14)$$

b) For the stable case, the solution for $K = \nu$ which satisfies the boundary condition (2.6) is

$$\theta' = c_2 \, \{(r\nu)^{-1/2} \tan^{-1}[(r\nu)^{1/2}(z-h)/(\nu+zh)] -$$

$$- [1/(2hr)] \, \ell n[(1+rz^2/\nu)/(1+rh^2/\nu)]\} \qquad (4.15)$$

c) For the unstable case the solution for $K = \nu^{-1/3} z^{4/3}$ which

---

[8] The notations a and b here are not to be confused with the same notations elsewhere.

satisfies (2.6) is

$$\theta' = -3c_2\{(z/\nu)^{-1/3}-(h/\nu)^{-1/3} + \\ + (r\nu)^{1/2}\tan^{-1}[(\nu^{1/3}r)^{1/2}(z^{1/3}-h^{1/3})/ \\ /[1+r(z\nu h)^{1/3}] + [1/(2hr)]\,\ell n[(1+r\nu^{1/3}z^{2/3})/ \\ /(1+r\nu^{1/3}h^{2/3})] \qquad (4.16)$$

Substituting the solutions (4.14), (4.15) and (4.16) into (2.7) for the neutral, stable and unstable cases respectively and combining the result with (3.1), the following generalized expression for C is obtained:

$$C = -\ell n(kx^2) + \lambda + \tau \qquad (4.17)$$

where[9]

$$x = (\nu)^{1/2}$$

$$\lambda = \begin{cases} (1+1/r-\rho)\,\ell n(1+\xi^2) + \rho\,\ell n(1+w^2), & r\neq 0,\ \sigma<\infty \\ (1+1/r)\,\ell n(1+\xi^2), & r\neq 0,\ \sigma=\infty \\ \nu + (1-\varepsilon/2)[(\sigma/\nu)^{\varepsilon/2}-(\nu/\sigma)^{1-\varepsilon/2}], & r=0,\ \sigma<\infty \\ \nu\ , \quad \text{(unstable case only)} & r=0,\ \sigma=\infty \end{cases} \qquad (4.18)$$

---

[9] The meaning of ρ here is not to be confused with the meaning of the same elsewhere.

$$\tau = \begin{cases} (2\varepsilon-1)\xi^{-\varepsilon}\tan^{-1}[(\xi-w)/(w\xi+1)] + 1.5(1-\varepsilon)\ . \\ \qquad . \ [(\nu/\sigma)^{1/2} - 1], & r\neq 0,\ \sigma<\infty \\ (1-2\varepsilon)\xi^{-\varepsilon}\tan^{-1}(\xi^{-1}) - 1.5(1-\varepsilon), & r\neq 0,\ \sigma=\infty \\ (2\varepsilon-1)[1-(\sigma/\nu)^{\varepsilon/2}], & r=0,\ \sigma<\infty \\ -3, \quad \text{(unstable case only)} & r=0,\ \sigma=\infty \end{cases} \tag{4.19}$$

and

$$\begin{aligned} \rho &= (1-\varepsilon/2)\ w^{\varepsilon-2}\xi^{-\varepsilon} \\ \xi &= (r\ \nu)^{1/2} \\ w &= (r\ \sigma)^{1/2} \\ \varepsilon &= \text{sign}\ (\mu_s) \end{aligned} \tag{4.20}$$

That the function C in (4.17) is not defined for $r = 0$ and $\sigma = \infty$ in the stable case is because the solution for θ' from (4.13) for these parameters does not satisfy the upper boundary condition (2.6). This is a consequence of the simple model $K \equiv \nu$ for $\nu \leq z \leq h$.

That the new expression for C in (4.17) is an improvement on the expressions in (4.10) and (4.11) will become apparent later on.

4.5. *Universal constants A, B and C for the neutral case* ($\mu_s = 0$)

In this section, expressions for the universal functions A, B and C when the stratification is neutral ($\mu_s = 0$) will be derived from the

generalized solutions for p and θ' in (2.25) and (4.13) respectively.

Thus solving (2.25) for C_1/C_2 and (4.14) for c_1/c_2 with the upper boundary conditions $p = \theta' = 0$ at $z = h = 1$ and combining the result with (3.1), the following expressions for A, B, and C are obtained:

$$\left.\begin{aligned} A &= 2\,\frac{bc - ad}{c^2 + d^2} \\ B &= -\ell n\, k + 2\,\frac{ac + bd}{c^2 + d^2} \\ C &= \ell n\,[(1+r)^{1+1/r}/k] \end{aligned}\right\} \quad (\mu_s = 0) \tag{4.21}$$

where

$$\left.\begin{aligned} a &= \sum_{n=0}^{\infty} (-1)^n\, \Phi_{2n}/[(2n)!]^2 \\ b &= \sum_{n=0}^{\infty} (-1)^n\, \Phi_{2n+1}/[(2n+1)!]^2 \\ c &= \sum_{n=0}^{\infty} (-1)^n/[(2n)!]^2 \\ d &= \sum_{n=0}^{\infty} (-1)^n/[(2n+1)!]^2 \end{aligned}\right. \tag{4.22}$$

and Φ_n is defined in (2.27). Since in this case ν is not defined, $\nu = 1$ is used. Then the expression for C in (4.21) can also be obtained by simply setting $\nu = \sigma = \varepsilon = 1$ in (4.17) - (4.20).

For $k = 0.35$ from (4.21) and (4.22) calculations yield the following values for the universal constants: $A(0) = 1.42$, $B(0) = 1.90$ and $C(0) = 2.44$ and $C(0) = 2.05$ for $r = 1$ and $r = 0$, respectively. The value of $r = 1$ is from subsection 5c where the

results of this investigation are compared with observations in Antarctica.

These values for A(0) and B(0) are to be contrasted with the values A(0) = 1.57 and B(0) = 2.99 reported in Zilitinkevich et al. (1967) in their Table 2. It is stated therein that the latter values are from Blinova and Kibel who derived them from the solution of Eq. (2.1) for the model of k = z throughout the BL as was the case in finding the solution (2.28). Since in both studies the same problem is solved, the natural conclusion would be that the solution should be exactly the same. However, it is difficult to conceive how the reported values in Zilitinkevich et al. (1967) came about unless their A and B have a different meaning, which does not seem to be the case.

In this study, it is seen that Euler's constant (mentioned in Zilitinkevich et al., 1967) is absorbed in the constants of integration C_1 and C_2 as in (2.25) and therefore does not appear in the expression for B(0). This is in contrast to the corresponding formula for B(0) in Zilitinkevich et al. (1967) where Euler's constant is included explicitly.

Other values for A(0), B(0) and C(0) that have appeared in the literature are summarized in Table I.

4.6. *'Smoothed' universal functions A, B and C*

After experimentation it was observed that the two branches--stable and unstable--of the universal functions A, B and C meet approximately at $\mu_s = 0$. Therefore, it seemed reasonable to fit a function to the two branches in the neighborhood of $\mu_s = 0$ so as to

make them "smooth" for all values of μ_s, and to facilitate the numerical solution of the system (3.7) - (3.9).

Thus the smoothed functions A, B and C expressed symbolically by a function, say, $F(\mu_s)$ read

$$F(\mu_s) = \begin{cases} a_3\mu_s^3 + a_2\mu_s^2 + a_1\mu_s + a_0, & \text{if } \mu_n \leq \mu_s \leq \mu_p \\ \text{A, B or C (before smoothing)}, & \text{if } \mu_s \leq \mu_n,\ \mu_s \geq \mu_p \end{cases} \tag{4.23}$$

For each one of the functions F = A, B or C the fitting consisted of determining the coefficients a_3, a_2, a_1 and a_0 and the knot points μ_n and μ_p (in the negative and positive branches of μ_s respectively) such that F and its derivative are continuous at these points. The universal functions A, B and C thus obtained for the parameters $\sigma = 1000$ and $\sigma = 10^{-1}$ in (4.2) for the stable and unstable cases respectively and for $r = 1$ in (4.17) - (4.20) can be summarized as follows:

$$A = \begin{cases} 5.107\cdot10^{-3}\mu_s^3 + 9.794\cdot10^{-2}\mu_s^2 + 6.247\cdot10^{-1}\mu_s + \\ \qquad + 1.5690, & \text{if } -6 \leq \mu_s \leq 1 \\ 0.7071\, x^{-1} + 0.7071\, x + 0.5\, x^2 - 0.3536\, x^3, & \text{if } \mu_s > 1 \\ 2.832\, x - 10\, x^2 + 9.656\, x^3, & \text{if } \mu_s < -6 \end{cases} \tag{4.24}$$

$$B = \begin{cases} 1.291\cdot10^{-3}\mu_s^{\,3} + 1.972\cdot10^{-4}\mu_s^{\,2} - 1.527\cdot10^{-1}\mu_s - \\ \qquad - 2.5461, & \text{if } -6 \leq \mu_s \leq 1 \\ -\ln(k\,x^2) - 0.7071\,x^{-1} + 1 + 0.7071\,x + \\ \qquad + 0.3536\,x^3, & \text{if } \mu_s > 1 \\ -\ln(k\,x^2) - 3 + 9.656\,x - 2.832\,x^3 + \\ \qquad + 4.25\,x^4, & \text{if } \mu_s < -6 \end{cases} \tag{4.25}$$

$$C = \begin{cases} -8.529\cdot10^{-3}\mu_s^{\,3} + 2.791\cdot10^{-2}\mu_s^{\,2} - \\ \qquad - 1.095\mu_s + 1.319 & \text{if } |\mu_s| \leq 1.5 \\ -\ln(k\,x^2) + (\tan^{-1}x - 1.43)\,x^{-1} + \\ \qquad + (2 - 0.0158\,x^{-1})\ln(1 + x^2), & \text{if } \mu_s > 1.5 \\ -\ln(k\,x^2) - 3 - 3(\tan^{-1}x - 3.470)x + (2 - \\ \qquad - 0.04743x)\ln(1+x^2) & \text{if } \mu_s < -1.5 \end{cases} \tag{4.26}$$

and also

$$h = \begin{cases} 31.62\,x, & \text{for } \mu_s > 0 \\ 1/(31.62\,x), & \text{for } \mu_s < 0 \end{cases} \tag{4.27}$$

$$x = (\nu)^{1/2}$$

The knot point values in (4.24) - (4.26) were determined by inspection of the shape of the theoretical curves as they approached $\mu_s = 0$. It should be noted here that the values of the parameters σ and r for the unstable case are to be used with caution, since further

experimentation with observations is necessary to confirm these values.

The values of a_o in (4.23) from (4.24) - (4.26) are in reasonable agreement with the values of A(0), B(0) and C(0) computed from (4.21) and (4.22) and summarized in Table I.

This completes section 4 and in the subsequent sections the smoothed functions A, B and C in (4.24), (4.25) and (4.26), respectively will be utilized in all the remaining calculations.

5. RESULTS

Once the A, B and C functions are established and before presenting the solutions of the system (3.7) - (3.9), a computation of $\lim \delta$ and $\lim \alpha$ for $\mu_s = \pm\infty$ from (3.22) and (3.26) respectively will be given first.

5.1. *Computation of* δ for $\mu_s = \pm\infty$ ($\psi << f/N$ or $\gamma = 0$)

In this case, because of the smallness of ψ, $a = 1$ is obtained from (B27). Upon substituting the analytical functions (4.6), (4.7) and (4.17) for A, B and C respectively into (3.22) and for constant σ as in (4.2), the following expression for δ is obtained:

$$\delta = -b\,[\tan^{-1}(I) + (\varepsilon - 1)\,\mathrm{sign}(I)\,\pi/2], \qquad (\psi \neq 0) \qquad (5.1)$$

where

$$I = \begin{cases} [(1-\varepsilon/2)r^{-1}\sigma^{\varepsilon/2-1}\cdot \ell n(1+w^2) + (1-2\varepsilon)r^{-\varepsilon/2}\tan^{-1}(\omega) + \\ \qquad + 1.5(1-\varepsilon)\sigma^{\varepsilon/2} - b_o]/a_o, & r\neq 0,\ \sigma<\infty \\ [(1-2\varepsilon)r^{-\varepsilon/2}\cdot \pi/2 - b_o]/a_o, & r\neq 0,\ \sigma=\infty \\ [(2-2.5\varepsilon)\sigma^{\varepsilon/2} - b_o]/a_o, & r=0,\ \sigma<\infty \\ -b_o/a_o, \quad \text{(unstable case only)} & r=0,\ \sigma=\infty \end{cases} \tag{5.2}$$

and

$$\begin{aligned} a_o &= [(1+\varepsilon)f + 9(1-\varepsilon)g]/2 \\ b_o &= [(1+\varepsilon)g - 9(1-\varepsilon)f]/2 \end{aligned} \tag{5.3}$$

The definition of ε is in (4.3), the definitions of f and g are in (4.6), of ω in (4.20) and the definition of b is in Appendix A. Moreover from (4.8) it is seen that $c = -1$ and $d = 0$ for $\sigma = \infty$.

The expressions for I in (5.2) for $r = 0$ and $\sigma = \infty$ and for their combinations with $r \neq 0$ and $\sigma < \infty$ are included only to contrast the results of this investigation with the results that would be obtained if the model in GM were instead adopted. The computation of δ from (5.1) - (5,3) for various values of σ and for both $r = 0$ and $r = 1$ are summarized in Table III. The value $r = 1$ was found in this investigation from a comparison of the results of this investigation with observations of α in the South Pole as reported in section 6.

5.2. *Computation of* α for $\mu_s = \pm\infty$ ($\psi = 0$)

In this case also, the substitution of the analytical functions

(4.6) and (4.7) for A and B into (3.26) gives the following expression for the cross-isobaric angle α, which is valid for σ constant in the range $0 < \sigma < \infty$:

$$\alpha = \left\{ \begin{array}{ll} -b \tan^{-1}(f/g) , & \text{if } \mu_s = +\infty \\ \text{complex} , & \text{if } \mu_s = -\infty \end{array} \right\} \quad (\psi = 0) \qquad (5.4)$$

Here α = complex means that the analytical functions for A and B do not fulfill the condition (3.24), i.e. $|A| > kR_o e^{-B}$ in the neighborhood of $\mu_s = -\infty$ and f and g are defined in (4.8). As in subsection 5a, examples of the computation of α from (5.4) for various values of σ are also summarized in Table III. The value of $\alpha_{+\infty} = 45$ deg for $\sigma = \infty$ coincides with Zilitinkevich and Monin's (1974) computation of $\alpha_{+\infty}$ from different A, B and C functions, and is positive because the computations are for the Southern Hemisphere. That $\alpha_{+\infty} = 45$ deg for $\sigma = 1000$ means that it is big enough for $\alpha_{+\infty}$ to approach its value at $\sigma = \infty$ very closely.

5.3. *Computation of the resistance and heat-transfer laws in the general case* (γ and $G \neq 0$, $\psi < \simeq 0.1$ and all χ)

Here solutions of the transcendental system (3.3) - (3.6) or equivalently (3.7) - (3.9) for the resistance and heat-transfer laws in the general case[10] of $0 \leqslant \psi \leqslant \simeq 0.1$, N (or γ) $\neq 0$, i.e. $a \neq 1$ (from B27), $G \neq 0$ and for all possible values of χ, are presented. For this purpose the 'smoothed' universal functions A, B and C in (4.24) -

---

[10] The symbol $\simeq$ in this connection means "an order of"

(4.26) and displayed in Fig. 3 are used. This undertaking was suggested in GM (subsection c.4) and the results of this subsection are therefore considered to be a follow-up of that paper since it is the first time such solutions are presented. It is found that the system (3.7) - (3.9) is sensitive to the choice of the A, B and C functions and that it can give multiple solutions for certain choices of the external parameters. Arya's A, B and C functions are an example of such a choice for which this system is sensitive as will be shown in the next section.

Although the system (3.7) - (3.9) was solved for both stable and unstable cases and for various combinations of the parameters N (or γ), R_o and S, for brevity the following discussions will be concerned only with the stable case solutions. The solutions for the unstable case will be dealt with in a separate investigation.

Solutions of the system (3.7) - (3.9) for α (or δ), μ_s, u_*/G and T_*/θ_o, in the Southern Hemisphere ($\phi < 0$), for the parameters f, N (or γ) typical of mid-latitudes, physically sound choices of the external parameters R_o and S and for $\psi = 2 \times 10^{-3}$ are presented in Figs. 4 - 13. First α and δ versus χ are displayed in Fig. 4 for $R_o = 10^7$ and for different values of S. From Fig. 4, it is seen that depending on the specific value of S, there are three types or regimes of solutions, namely: a) regime-1 for $S < S_c$ (S_c is a certain critical value) the behavior of α is of the 'oscillatory' type, b) for $S > S_c$ of the 'staircase' type and c) for $S = S_c$ of the 'transition' type for $S = S_c$, which can either be of the 'extreme oscillatory' (for $S = S_c-$) or 'extreme staircase' (for $S = S_c+$) types. The behavior of δ in all three regimes is reversed. The critical value S_c is seen to lie

between S_c- = 701.470 and S_c+ = 701.475. This sub-division of the solutions into three regimes will occur if instead S is fixed and ψ is allowed to vary from lower to higher than its critical values, since either process gives origin to the same physical cause.

From the shapes of α and/or δ in Figs. 4 and 5, it is quite clear that in the 'oscillatory' regime the surface wind $\underline{V}_s$ must follow the geostrophic wind $\underline{G}$ around the clock; first at a slower rate than $\underline{G}$ until $\alpha = \alpha_{max}$, then at a faster rate so as to 'catch up' with $\underline{G}$ until $\alpha = \alpha_{min}$ and then at a slower rate again to complete the cycle. In the 'staircase' regime, on the other hand, it is seen from the shapes of α and/or δ that (assuming the 'starting point' $\chi = 0$) first $\underline{V}_s$ follows $\underline{G}$ up to $d\alpha/d\chi = 1$ or $\delta = \delta_{max}$ (i.e., $d\delta/d\chi = 0$), then $\underline{V}_s$ retrocedes getting farther and farther away from $\underline{G}$ until once again $d\alpha/d\chi = 1$ or $\delta = \delta_{min}$ and finally $\underline{V}_s$ again follows $\underline{G}$ to complete the cycle. In other words, when $\underline{V}_s$ follows $\underline{G}$ around the clock, the regime is 'oscillatory'; whereas when $\underline{V}_s$ follows $\underline{G}$ and then 'chooses' to stay where it is, the regime is of the 'staircase' shape.

In the 'transition' regime the rapid change of α (as seen in Fig. 4c at S_c- = 701.470) from near 225 deg to near -135 deg (passing through $\alpha = 0$) in such a small interval of χ is also possible to understand (with a little imagination) if the effect of all forces acting on $\underline{V}_s$, not only to change its direction but also to reduce its magnitude, is taken into account. Moreover, a distinctive feature of the 'transition' regime is that the system (3.7) - (3.9) yields multiple solutions (not shown here), which then disappear as S becomes less or greater than S_c. Another feature is that μ_s attains very large values. Calculations indicate that the value of μ_s at $S = S_c$ must be extremely large, since the value for S_c- = 701.470 or S_c+ = 701.475 at

χ = 225.4 deg is already of order 10^5.

The physical cause for the existence of the three regimes must be due to the relative influence of the pressure gradient force (together with the Coriolis and frictional forces) on the surface wind in comparison with the influence of the gravity force (parallel to the sloping surface) as the value of S (or equivalently ψ) increases from a subcritical to a supercritical value.

The solutions for μ_s, α, u_*/G and T_*/θ_o in the 'oscillatory' and 'staircase' regimes for $\psi = 2 \times 10^{-3}$ and for three different values of R_o and S are presented in Figs. 6 - 9 and 10 - 13, respectively. The corresponding solutions for the case when $\psi = 0$ are shown in the same figures by the horizontal lines.

The marked influence not only of the terrain slope (even when it is of an order as small as 10^{-3}) but also of the orientation of the geostrophic wind (from the FLV) on the momentum and heat transfers in the BL above sloping terrain as compared to the transfers for the case when the underlying surface is horizontal can be clearly seen and appreciated from the figures. As to the influences of R_o and S, it is also evident from the figures that the larger R_o and S are, the stronger the influences will be. The other peculiarities of the solutions are left up to the reader's imagination,

As to the influence of S on the solutions, from Fig. 5a, it is seen that as the value of S increases from 300 to 1100, first the maxima and minima in the curves of α (in the 'oscillatory' regime) become steeper and steeper as they approach the 'transition' regime, becoming steepest right at the 'transition'. After this, the curves correspond to the 'staircase' regime where a further increase in S

makes the curves approach a straight line, i.e., $\alpha = \chi +$ constant. The behavior of δ in the reversed sense is evident from Fig. 5b.

6. COMPARISON WITH OBSERVATIONS

In this section a comparison of the results of this investigation with observations will be presented. The meteorological measurements taken at the Amundsen Scott station in the South Pole (ϕ = -90 deg) in 1958 are chosen for this purpose. These observations were analyzed by Dalrymple et al. (1966) for the sunless period (sun below the horizon), March 22 -September 24, 1958 and data on the cross-isobaric inflow angle α are now presented as a function of the direction of the geostrophic wind (from N) in their Table 5. These data have been discussed in other contexts by e.g. Lettau and Schwerdtfeger (1967), Neff (1981) and Radok (1981).

To carry out the comparison, it was first necessary to determine the intensity and direction of the large scale terrain slope at the South Pole (i.e., representative at a scale of an area of about 1000 km radius). Except for Dalrymple et al. (1966), other previous investigators simply estimated either the intensity and/or the direction of the surface slope at the South Pole. From four traverses and distances of 200 - 300 km from the South Pole, Dalrymple et al. computed an average slope angle of 1.76×10^{-3} rad with the FLV directed towards the Weddell Sea from 152 deg East of the Greenwich meridian. Bently (1971) in his studies of gravity increase at the South Pole estimated the local surface slope direction (or FLV) to be from 80 deg East meridian, but no estimate of the slope intensity was reported. Radok (1983) from an analysis of wind and surface elevation measurements during a 30 km vehicular run towards 80 deg East concluded that the

local terrain upslope direction is indeed towards 80 deg East. Also from the surface elevation profile along 80 deg East from the South Pole (his Fig. 4), the local intensity of the slope is about 1.2×10^{-3} rad. In a more recent study McInnes and Radok (1984) have constructed surface elevation contour lines for the Antarctic plateau from the Soviet Atlas of Antarctica, which extends from the South Pole up to 980 km. From this, it is seen that the FLV through the South Pole (drawn orthogonally to the contour lines) is approximately from 80 deg East. Also an estimate of the slope intensity from their Fig. 2 gives a value of about 3.0×10^{-3}.

Since the above calculated or estimated values of the surface slope intensity and direction, except for that of McInnes and Radok, are of local nature, an attempt was made to independently determine the intensity and direction of the surface slope at the South Pole. From an analysis of recent topographic maps of Antarctica prepared by the Scott Polar Research Institute of the University of Cambridge (Drewry, 1983), the estimated values of these two parameters (in good agreement with the above mentioned values, but in contrast with the average slope direction of Dalrymple et al.) are respectively $\psi = 2.5 \times 10^{-3}$ rad and directed downwards towards 240 deg from Greenwich meridian taken as North. A method to calculate ψ and the direction of the FLV is also given in Appendix B.

As to the other input external parameters for the model, estimates from Dalrymple (1966), representative at a horizontal scale of the order of 1000 km or more around the South Pole, yield: $\gamma = 10^{-2}$ ^{o}C/m, $\theta_m = 220$ K, $z_o = 1$ mm, and $\bar{G} = 8.2 \pm 2.4$ m/s. This average value was computed from the "3-value running" means of G in Dalrymple's (1966) Table 10. From these parameters, the computed

surface Rossby number R_o [= $G/(fz_o)$], is 6×10^8. Because no direct measurements of θ_o [= $(\theta - \Theta)$ at $z = z_o$], i.e., the value of the temperature difference between the temperature inside and outside the BL at z_o = 1 mm, are available, to compute θ_o a value for the external stability parameter S at the South Pole S = 800 was assumed. From this value and the parameters specified above, the value of θ_o, from $\theta_o = -SfG/\beta$ ($\beta = g/\Theta_m$), is -21.4^oC. This and the other values seem to be realistic representative values at the South Pole at a horizontal scale of 1000 km or more according to Lettau and Radok (personal communication).

The frequency distribution of the observed α versus χ (direction from the FLV of the geostrophic wind) in a slightly different arrangement than in Dalrymple et al. `(1966), is given in Table II. A comparison of these data points with the theoretical results of α as a function χ found in this investigation and for the parameters S = 800, $R_o = 6 \times 10^8$, $\psi = 2.5 \times 10^{-3}$ rad, $\gamma = 1 \times 10^{-2}$ $^oC/m$ and Θ_m = 220 K is shown in Figs. 14 and 15. In order to be able to make possible the comparison at *any interval* in χ, the curves in Figs. 14 and 15 are plotted over two cycles. The solid curves represent the results when the A, B and C functions of this investigation are used and the dot-dashed curves represent the results when Arya's A, B and C functions are used. Fig. 14 shows a comparison of the theoretical results against the frequency distribution of the data points presented in Table II as a function of χ. Fig. 15 shows a comparison of theoretical results with observations, where each data point is computed as a '3-column running' mean of the data points in Fig. 14 (or in Table II), taking into account the corresponding frequencies as weight factors.

In the '3-column running' mean computation, two of the data points, namely: α = 22 deg for χ = 218 deg and α = 90 deg for χ = 240 deg (Table II), which were seen to fall completely off the main trend were removed. Figs. 16 - 18 show the solutions for μ_s, u_*/G and T_*/θ_o respectively, for the same choice of all external parameters and in a similar format as in Figs. 14 and 15. A comparison of these results with observations is not possible since no measurements of these parameters were carried out during the South Pole expedition of 1958.

From Figs. 14 and 15, it is clear first of all that the overall agreement between the observed and the theoretical curves throughout the whole cycle is surprisingly good, considering the simplicity of the theory. The agreement with the dot-dashed curve is also good in the intervals, $0 \leqslant \chi \leqslant 152.15$ deg and $\chi > 281.13$ (where $\mu_s \leqslant 82.76$ and $\mu_s \leqslant 85$ respectively). This is precisely the interval where Arya's A, B and C functions are well-behaved. Next, it is also clear from Figs. 14 and 15 that both the theoretical and the observed curves of α correspond to the solutions of the 'staircase' regime, which as discussed above occurs when S exceeds a critical value, S_c. From the parameters of the problem in this particular example, it is found that $S_c = 574$.

In Figs. 14 - 18 the dotted portion of the dot-dashed curves in the interval $115.42 < \chi < 281.13$ deg is the interval where $\mu_s > 85$ and therefore Arya's A, B and C functions cease to be useful and are included only to satisfy the scientific query of what would the results be like if Arya's functions were used beyond the limit in which they are properly behaved. Further inspection of the dot-dashed curves in Figs. 14 - 18 reveals that: (1) in the intervals $0 \leqslant \chi \leqslant 152.15$ deg and $\chi \geqslant 281.13$ deg, where $\mu_s \leqslant 82.76$ and $\mu_s \leqslant 85.00$

respectively (Fig. 16), α is continuous; (2) in the interval $152.15 < \chi < 281.13$ deg where $\mu_s > 85$ in the whole interval and therefore Arya's functions are no longer useful discontinuities in α and μ_s at $\chi = 152.15$ deg occur (Figs. 15 and 16); (3) in the interval $115.42 < \chi < 152.15$ deg, the existence of multiple solutions is evident (Figs. 15 - 18). Also in this investigation it is found that the computed value of h from the first expression in (4.27) is in reasonable agreement with the average value of the measured inversion heights reported by Dalrymple et al. (1966).

Finally, a closer look at Fig. 15 reveals that the theoretical curve and the data points differ in detail thus leaving room for improvements and/or further tests of the theory with observations. For example, in the interval approximatèly $0 < \chi < 40$ deg, the observed data points show a tendency to flatten out very sharply. At present, it is not clear what the reasons for this behavior are. It may be that the '3-column running' mean is not the proper way to represent these data or it could also be that the data is not perfect in this interval. The fit in the inverval $0 < \chi < 40$ deg was slightly better (not shown) if in lieu of the '3-column running' mean the '3-value running' mean of the column means or simply the column means was used for the comparison. However, as already mentioned, in this preliminary test no exhaustive experimentations with data, for example with somewhat different values of the input external parameters, are attempted. This will be a topic for a separate investigation. The point to be borne in mind from Figs. 14 and 15 is the interesting finding that the present theory is capable of reproducing the observed *shape* of the curve α versus χ, although the more precise comparison of the two

curves at any interval in χ will depend on the more accurate determination, for example, of the external parameter S.

7. CONCLUSIONS AND FUTURE OUTLOOK

An extension of the model in GM for the BL above sloping terrain, to include not only a more general expression for the 'eddy' viscosity or diffusivity coefficient K that depends on both the internal stability μ_s and height z to an arbitrary power, but also the stability dependent depth, $h\ (\mu_s)$, of the BL as an additional parameter in the spirit of the papers by Zilitinkevich (1972) and Zilitinkevich and Monin (1974) is presented. From this model, analytical expressions for the mean wind and temperature structures in the BL which are also known as the velocity--and temperature--defect profiles in the context of the Rossby-number similarity theory for the BL above sloping terrain are derived. It is seen that these profiles depend not only on μ_s and z, but, through the lower boundary conditions also on the other parameters of the problem namely: the surface Rossby number R_o and the external stability parameter S in addition to the slope angle ψ and the angle χ the geostrophic wind makes with the FLV.

Next, as by-products of these solutions on the one hand, analytical expressions for the universal functions A, B and C of the Rossby-number similarity theory (for the same functional form of K as in GM) are found. In analogy with the A, B and C functions of the BL above a horizontal surface, these functions are also functions of μ_s alone. A comparison with the corresponding functions in GM shows that the former functions are a generalization of the latter not only to

include additional terms, but also to include h as an independent parameter. On the other hand, as a consequence of the asymptotic formula $K = z$ (which is equivalent to the logarithmic asymptotes) in the dynamic sublayer, a system of transcendental equations for the geostrophic drag u_*/G and heat-transfer T_*/θ_o coefficients and the cross-isobaric inflow angle α is derived. This system is closed in the sense that there are four equations for four unknowns u_*/G, T_*/θ_o, α and μ_s (for a given set of the external parameters R_o and S and the angles ψ and χ) and corresponds to the resistance and heat-transfer laws of the Rossby-number similarity theory for the BL above sloping terrain.

Furthermore it is seen that the shapes of the universal functions A, B and C depend on the solutions for the mean wind and temperature structures in the whole BL and therefore on the specific model equations, the form of K, and the boundary conditions used; whereas the expressions for the resistance and heat-transfer laws depend only on the logarithmic asymptotes near the ground. From this, the interesting conclusions are that any theory which yields these same asymptotic formulas should also yield the same resistance and heat-transfer laws and that different theories will give different A, B and C functions.

As a further step in the improvement of these functions, Laikhtman and Kurdova's (1980) suggestion for the heat-flux profile in the BL, which allows for three free parameters is followed-up and generalized to include h as an additional parameter. Two of these free parameters are connected with the boundary conditions and the third parameter allows for the heat-flux profile to have a curvature. From this, an equation for the temperature distribution is derived. From

the solutions of this equation for the same functional form of K as in GM, analytical expressions for the universal function C are obtained. This new C function is found to be more realistic than the previous one and is therefore used in all the calculations.

For the universal functions A, B and C thus determined, first three special solutions of the transcendental system (3.7) - (3.9) are presented. Two of these solutions have much relevance in Arctic or Antarctic applications. For the special case of G = 0 and $\psi \ll f/N$ (or $\gamma = 0$) *explicit* expressions for the surface drag $u_*/\tilde{U}$ coefficient, and the direction (from the FLV) of the surface wind δ and T_*/θ_o are obtained when the stability μ_s is known. For the other special case of a very large μ_s (i.e. in the limit of $\mu_s = \pm\infty$) and $\psi \ll f/N$ (or $\gamma = 0$), *explicit* expressions for the angles $\delta_{\pm\infty}$ and $\alpha_{\pm\infty}$ ($\alpha_{\pm\infty}$ is for the case when $\psi = 0$) are derived and found to depend only on the universal functions A, B and C or A and B respectively, i.e., ultimately only on μ_s. For the A, B and C functions found in this investigation, the numerical values of these angles for r = 0 and r = 1 and for various values of σ are summarized in Table III.

Next, numerical solutions of the transcendental system for α (or δ), μ_s, u_*/G, T_*/θ_o as a function of χ, for many combinations of the external parameters R_o and for S and ψ in the range $0 \leq \psi \leq \simeq 0.1$ (see footnote 10) are obtained. From this, an interesting and novel result is the finding that there are three different types of solutions depending on whether S (or ψ) is less than, equal to or greater than a certain critical value S (or ψ_c), which depends on the other parameters. The solutions for $S < S_c$ are of the 'oscillatory' type, for $S > S_c$ of the 'staircase' type and for $S = S_c$ of the 'transition' type, can either be of the 'oscillatory transition' ($S = S_c-$) or

'staircase transition' ($S = S_c+$) types. The behavior of α and δ in the three regimes is displayed in Figs. 4 and 5 and a physical picture for this behavior of the surface wind with respect to the geostrophic wind is offered.

Diagrams of the solutions for α (or δ), μ_s, u_*/G and T_*/θ_o for both 'oscillatory' and 'staircase' types, $\psi = 2\times10^{-3}$ rad, three different values of R_o and S (for the stable case only) and values of the Coriolis parameter f and Brant-Väisälä frequency N typical of the mid-latitudes are displayed in Figs. 6 - 9 and 10 - 13 respectively. From these figures, it is seen that there is an appreciable influence not only of ψ but also of χ on the momentum and heat transfers in the BL as compared to the transfers (denoted by horizontal lines) for the case when the BL is above a horizontal surface.

As a preliminary test of the results of this investigation with observations, a comparison of the theoretical values of α with data values analyzed by Dalrymple et al. 1966) from the observations in the South Pole is displayed in Figs. 14 and 15. The figures show that α versus χ is of the 'staircase' type and that a comparison between the observed and theoretical curves is surprisingly good and therefore encouraging for further research along the lines of the present theory. Further comparisons of the results of this theory with observations not only in the stable case, but especially in the unstable case (not shown here) are left as a topic for a separate study. Such comparisons are essential to remedy or improve some of flaws of this theory.

The following are extensions of this theory that can be considered as topics of separate research: a generalization of theory

to include the physical height of the BL as an independent parameter in the spirit of the papers by Zilitinkevich and Deardorff (1974), Melgarejo and Deardorff (1974) and Zilitinkevich and Monin (1974); the re-evaluation of the universal functions A, B and C from data in the light of the system (3.3) - (3.6) a generalization of the theory to include baroclinicity as an additional external parameter, etc. In conclusion it is hoped that this paper will serve as a guide in the planning of future observational expeditions to provide information as to what type of data or parameters to collect, especially in such remote and perilous sites as Arctic and Antarctic regions. This would make it possible to critically test the validity of the present and various other theories in vogue today.

ACKNOWLEDGEMENTS

I wish to express my gratitude to the following people and Institutions who have played an important part in the outcome of this work. To Professor T. N. Krishnamurti, I am grateful for his kindness to invite me to spend one year at the Department of Meteorology of the Florida State University (FSU) where this work was initiated and for providing me with financial and computer support through NSF grant No. ATM 7819363. To Professor Albert Barcilon, I would like to express my gratitude for inviting me to spend one year at the Geophysical Fluid Dynamics Institute (GFDI) of FSU, where the major part of this work was carried out, and also for providing computer time during the first four months of my stay at GFDI. To Professor Richard Pfeffer, I would also like to express my gratitude for providing me with computer support for the completion of this work through the Office of Naval Research under Contract N00014-0265 and through the Computing Center at FSU. To Naturvetenskapliga Forskningsrŕdet (the Swedish Natural Science Research Council), I am very grateful for granting me a post-doctoral fellowship for two years to spend at FSU under contracts G-PD 4866-100 and G-GU 4866-101. To my wife, Olivia, I am especially grateful for her patience and understanding during the development of this work and for her skilful typing of the manuscript. Finally to all the many people of FSU and Tallahassee, I wish to express my appreciation and gratitude not only for their friendship and collaboration but also for their "gemütlichkeit," which made it possible to spend two and a half unforgettable years in Tallahassee.

APPENDIX A

List of Symbols

a = $1/[1 + (N\psi/f)^2]^{1/2}$ (external parameter)

A, B, C universal functions of μ_s

b sign ϕ = $+1$ if $\phi \geq 0$; -1 if $\phi < 0$

c_i real constants of integration in (2.26) for $i = 1,2,3$

c_p specific heat of air at constant pressure

C_i complex constants of integration in (2.25) for $i = 1,2,3$

f modulus of the Coriolis parameter $\tilde{f}$ ($= 2\,\Omega \sin\phi$)

g acceleration of gravity

G modulus of geostrophic wind $\underline{G}$ (external parameter)

h height of the BL (function of μ_s alone)

H sensible heat flux at the surface

i = $(-1)^{1/2}$

k von Kármán constant (set to 0.35 in the computations, Businger et al., 1971)

K, K_H vertical and horizontal turbulence coefficients, respectively

$\bar{K}$, $\bar{K}_H$ the same as K, K_H but for the undisturbed fields

L Monin-Obukhov length scale

$\tilde{L}$ latent heat of condensation

N Brunt-Väisälä frequency (external parameter)

q specific humidity of the total field

Q specific humidity of the undisturbed field

Q_r radiation component of heat flux

r free parameter in (4.12) set to one in the computations

R gas constant for air

R_o surface Rossby number

S stability parameter of the undisturbed field (external parameter)

T absolute temperature of the total flow

$\bar{T}$ absolute temperature of the undisturbed flow

T_* friction temperature

u_* friction velocity

u v w x, y, z wind components of the total field (Fig. 1a)

U V W x, y, z wind components of the undisturbed field (Fig. 1a)

z_o roughness length (external parameter)

α cross-isobaric inflow angle

α_H^o inverse of the turbulent Prandtl number (set to 1.35 in the calculations, Businger et al. 1971)

β $= g/\theta_m$, buoyancy coefficient (external parameter)

β_u empirical constant (set to 8 in the calculations)

γ $= d\theta/dz$ lapse rate of the undisturbed field (external parameter)

δ direction of surface wind from the FLV positive in counterclockwise direction (independent of either Northern or Southern Hemispheres)

$$\varepsilon = \text{sign}\,(\mu_s) = \begin{cases} +1 & \text{if } \mu_s \geq 0 \\ -1 & \text{if } \mu_s < 0 \end{cases}$$

ζ_u empirical constant (set to -0.22 in the calculations)

θ potential temperature of the total field

Θ potential temperature of the undisturbed field

Θ_m characteristic value of the potential temperature (set to 220 the in the calculations)

Θ_s surface value of Θ

λ_s length scale for the BL above sloping terrain

μ_s internal stability parameter (s denotes sloping terrain)

ρ air density of the total field

ρ_o air density of the undisturbed field

σ empirical constant set to 1000 for $\mu_s > 0$ and to 0.1 for $\mu_s < 0$

τ modulus of surface stress vector

ν an internal parameter proportional to $1/\mu_s$, defined in (2.17)

ϕ latitude angle ($\phi < 0$ in the Northern Hemisphere and $\phi > 0$ in the Southern Hemisphere)

Φ rate of liquid-phase formation

χ direction of G from the FLV

ψ terrain slope angle in radians

ω total vertical velocity in the transformed (ξ, η, ζ)-system

Ω = $7.292.10^{-5}$rad/s, the earth's rotation rate

$'$ over a letter denotes a BL or MS field variable

Abbreviations

BL boundary layer

deg degrees of an arc

FLV Fall-line vector (or $\hat{x}$-axis in Fig. 1a)

GM Gutman and Melgarejo (1981)

MS mesoscale

rad radians

APPENDIX B

Derivation of the Eqs. (1) and (2) of the main text and of the equations for the slope angle and direction

In deriving Eqs. (1) and (2) of the main text, the method put forward by Gutman (1969) and more recently e.g. by Panofsky and Dutton (1984) will be followed to obtain expressions for the BL or mesoscale (MS) fields as deviations from their respective basic "undisturbed" (or background) fields. To begin, the model equations for the total turbulent atmospheric flow after applying the Reynolds averaging process can be quite generally presented as,

$$
\begin{aligned}
&\frac{du}{dt} - \tilde{f} v = \frac{-\theta}{\theta_m}\frac{\partial \pi}{\partial x} + \Delta u \\
&\frac{dv}{dt} + \tilde{f} u = \frac{-\theta}{\theta_m}\frac{\partial \pi}{\partial y} + \Delta v \\
&\frac{dw}{dt} + g = \frac{-\theta}{\theta_m}\frac{\partial \pi}{\partial z} + \Delta w \\
&\frac{d\theta}{dt} = \frac{\tilde{L}}{c_p}\Phi + Q_r + \Delta\theta, \qquad \theta = T(1000\ \mathrm{mb}/p)^{R/c_p} \\
&\frac{dq}{dt} = -\Phi + \Delta q, \qquad \pi = (c_p\Theta_m/\theta)T \\
&\frac{d\rho}{dt} = -\left(\frac{\partial u}{\partial x} + \frac{\partial v}{\partial y} + \frac{\partial w}{\partial z}\right)\rho, \qquad p = \rho RT
\end{aligned}
\tag{B1}
$$

where

$$
\frac{d}{dt} = \frac{\partial}{\partial t} + u\frac{\partial}{\partial x} + v\frac{\partial}{\partial y} + w\frac{\partial}{\partial z}
$$

$$
\Delta = \frac{\partial}{\partial x}K_H\frac{\partial}{\partial x} + \frac{\partial}{\partial y}K_H\frac{\partial}{\partial y} + \frac{\partial}{\partial z}K\frac{\partial}{\partial z}
$$

and t is time; the x, y and z axes form a right-handed system of Cartesian coordinates with the x and y axes having an arbitrary orientation in the horizontal plane and the z axis directed upward; u,

v and w are respectively the components of wind vector along these axes; θ is the potential temperature and q the specific humidity. The terms associated with the operator Δ are a parameterization via the 'eddy' exchange or K hypothesis of the Reynolds stress, heat- and moisture flux terms that result from applying the averaging process. K_H and K are the horizontal and vertical turbulence coefficients, respectively, which at this point are assumed to be the same for momentum, heat and moisture transports. The other notations are in Appendix A or are standard in meteorological parlance.

The concept of undisturbed fields of meteorological elements, i.e., fields which would exist in the absence of BL or MS disturbing factors (such as orographic and thermal inhomogeneities, etc.) is introduced by assuming that all meteorological variables can be decomposed in the undisturbed part and the BL or MS part, which will be denoted by capital letters (sometimes by capital letters with a _ or a o) and primes, respectively. That is,

$$
\begin{array}{lll}
\theta = \Theta + \theta', & p = P + p', & \rho = \rho_o + \rho' \\
T = \bar{T} + T', & q = Q + q', & \pi = \Pi + \pi' \\
u = U + u', & v = V + v', & w = W + w' \qquad\qquad (B2) \\
|\theta'| \ll \Theta, & |p'| \ll P, & |\rho'| \ll \rho_o \\
|T'| \ll \bar{T}, & |q'| \ll Q, & |\pi'| \ll \Pi, \quad |\theta - \Theta_m| \ll \Theta_m
\end{array}
$$

Observations show that the above inequalities are satisfied in all BL or MS processes. It is natural to think that the undisturbed fields must coincide with the large-scale circulation, such as that calculated by the current weather forecast methods. From (B2) it is also seen that in the absence of BL or MS disturbances, the

undisturbed fields must satisfy the system (B1) identically. Thus the equations for the undisturbed fields can be presented as,

$$
\begin{aligned}
&\frac{DU}{Dt} - \tilde{f}\,V = \frac{-\theta}{\theta_m}\frac{\partial \Pi}{\partial x} + \bar{\Delta}U \\
&\frac{DV}{Dt} + \tilde{f}\,U = \frac{-\theta}{\theta_m}\frac{\partial \Pi}{\partial y} + \bar{\Delta}V \\
&\frac{DW}{Dt} + g = \frac{-\theta}{\theta_m}\frac{\partial \Pi}{\partial z} + \bar{\Delta}W \qquad\qquad (B3) \\
&\frac{D\rho_o}{Dt} = -\left(\frac{\partial U}{\partial x} + \frac{\partial V}{\partial y} + \frac{\partial W}{\partial z}\right)\rho_o, \qquad P = \rho_o R\bar{T} \\
&\frac{D\theta}{Dt} = Q_r + \bar{\Delta}\theta, \qquad \theta = T(1000\ \text{mb}/P)^{R/c_p} \\
&\frac{DQ}{Dt} = \bar{\Delta}Q, \qquad \Pi = (c_p\theta_m/\theta)\bar{T}
\end{aligned}
$$

where

$$
\begin{aligned}
&\frac{D}{Dt} = \frac{\partial}{\partial t} + U\frac{\partial}{\partial x} + V\frac{\partial}{\partial y} + W\frac{\partial}{\partial z} \\
&\bar{\Delta} = \frac{\partial}{\partial x}\bar{K}_H\frac{\partial}{\partial x} + \frac{\partial}{\partial y}\bar{K}_H\frac{\partial}{\partial y} + \frac{\partial}{\partial z}\bar{K}\frac{\partial}{\partial z}
\end{aligned}
$$

In deriving (B3) for simplicity the phase-transitions of water vapor are neglected by setting $\Phi = 0$. Further simplifications in (B3) can be introduced e.g by noting that the terms $D\ln\rho_o/Dt$ and W are known to be small compared to their corresponding values in BL or MS processes. In most practical applications, the undisturbed meteorological fields will be required to satisfy simpler relations than in (B3). In the present investigation the undisturbed fields of wind and temperature will be assumed to be in geostrophic equilibrium and linearly increasing with height, respectively. Substituting the definitions (B2) into (B1), subtracting (B3) from the result and neglecting the small terms, the following equations are arrived at:

$$\frac{du'}{dt} + u'\frac{\partial U}{\partial x} + v'\frac{\partial U}{\partial y} + w'\frac{\partial U}{\partial z} - \tilde{f}\,v' = -\frac{\partial \pi'}{\partial x} + \Delta u' + \tilde{\Delta} U$$

$$\frac{dv'}{dt} + u'\frac{\partial V}{\partial x} + v'\frac{\partial V}{\partial y} + w'\frac{\partial V}{\partial z} + \tilde{f}\,u' = -\frac{\partial \pi'}{\partial y} + \Delta v' + \tilde{\Delta} V$$

$$\frac{dw'}{dt} + u'\frac{\partial W}{\partial x} + v'\frac{\partial W}{\partial y} + w'\frac{\partial W}{\partial z} - \beta\,\theta' = -\frac{\partial \pi'}{\partial z} + \Delta w' + \tilde{\Delta} W$$

$$\frac{d\theta'}{dt} + u'\frac{\partial \Theta}{\partial x} + v'\frac{\partial \Theta}{\partial y} + w'\frac{\partial \Theta}{\partial z} = \frac{\tilde{L}}{c_p}\Phi + \Delta\theta' + \tilde{\Delta}\Theta \qquad \text{(B4)}$$

$$\frac{dq'}{dt} + u'\frac{\partial Q}{\partial x} + v'\frac{\partial Q}{\partial y} + w'\frac{\partial Q}{\partial z} = -\Phi + \Delta q' + \tilde{\Delta} Q$$

$$\frac{\partial u'}{\partial x} + \frac{\partial v'}{\partial y} + \frac{\partial w'}{\partial z} = \sigma' w, \quad \sigma' = \frac{g - R\gamma''}{R\Theta_m} = \text{const}, \quad \gamma'' = -\frac{\partial \bar{T}}{\partial z}$$

$$\frac{T'}{\bar{T}} = \frac{\theta'}{\Theta} + \frac{\pi'}{\Pi}, \quad \frac{p'}{P} = \frac{c_p}{R}\frac{\pi'}{\Pi}, \quad \frac{\rho'}{\rho_o} = \frac{p'}{P} - \frac{T'}{\bar{T}}$$

where

$$\tilde{\Delta} = \frac{\partial}{\partial x}(K_H - \bar{K}_H)\frac{\partial}{\partial x} + \frac{\partial}{\partial y}(K_H - \bar{K}_H)\frac{\partial}{\partial y} + \frac{\partial}{\partial z}(K - \bar{K})\frac{\partial}{\partial z}$$

and $\beta = g/\Theta_m$ is the bouyancy parameter. It is seen that Eqs. (B4) are quite general and therefore can be regarded as applying to most BL phenomena occurring in nature. In this investigation only a special form of (B4) will be considered. That is the case where the undisturbed flow can be assumed to be constant and in geostrophic equilibrium and the undisturbed potential temperature linearly increasing with height and in equilibrium with the motion. On the other hand, the BL or MS flow will be assumed to be incompressible and in hydrostatic balance, with horizontal scales much larger than vertical scales by at least an order of magnitude such that the simplifications of 'shallow convection' can be utilized. Finally the usual BL approximation whereby the vertical eddy coefficient for heat is larger than that for momentum by a the constant factor α_H^o will be

introduced. These considerations can be summarized as,

$$\tilde{f}\,U = -\frac{\theta}{\theta_m}\frac{\partial \Pi}{\partial y}, \qquad \tilde{f}\,V = \frac{\theta}{\theta_m}\frac{\partial \Pi}{\partial x}, \qquad W = 0$$

$$\theta(z) = \theta_s + \gamma z, \qquad \gamma = d\theta/dz = \text{const}$$

$$\frac{T'}{\bar{T}} = \frac{\theta'}{\theta} = -\frac{\rho'}{\rho_o}, \qquad K_{heat}/K_{momen} = \alpha_H^o \tag{B5}$$

$$\frac{\partial}{\partial x} K_H \frac{\partial}{\partial x} \text{ and } \frac{\partial}{\partial y} K_H \frac{\partial}{\partial y} \ll \frac{\partial}{\partial z} K \frac{\partial}{\partial z}$$

Also because information on turbulence pertaining to $\bar{K}$ is incomplete, the simplifying assumption that $\bar{K} = K$ will be used. This consideration together with (B5) reduces (B4) to,

$$\frac{du'}{dt} - \tilde{f}\,v' = -\frac{\partial \pi'}{\partial x} + \frac{\partial}{\partial z}\left(K \frac{\partial u'}{\partial z}\right)$$

$$\frac{dv'}{dt} + \tilde{f}\,u' = -\frac{\partial \pi'}{\partial y} + \frac{\partial}{\partial z}\left(K \frac{\partial v'}{\partial z}\right)$$

$$\frac{d\theta'}{dt} + w'\gamma = \frac{\partial}{\partial z}\left(\alpha_H^o K \frac{\partial \theta'}{\partial z}\right) \tag{B6}$$

$$\frac{\partial u'}{\partial x} + \frac{\partial v'}{\partial y} + \frac{\partial w'}{\partial z} = 0, \qquad \frac{\partial \pi'}{\partial z} = +\beta\theta'$$

Before seeking special solutions to (B6), next rather general transformation expressions will be developed to carry out the transformation from the (x,y,z)-system in the horizontal plane to the new terrain-following (ξ,η,ζ)-system, such that the lowest ζ-constant surface (i.e., $\zeta = 0$) coincides with the profile of the terrain $z = z_s(x,y)$ which makes small angles of inclination with the horizontal plane. Because of the smallness of the slope angle the approximations $\xi \simeq x$ and $\eta \simeq y$ will be used (Fig. 1a). Thus with the following simplified definition for the mapping

$$\xi = x$$

$$\eta = y \qquad \text{(B7)}$$

$$\zeta = \zeta(x,y,z) \quad \text{or} \quad z = z(x,y,\zeta)$$

and a straightforward application of the chain rule for partial differentiation, the following transformation expressions are derived

$$\left(\frac{\partial \alpha}{\partial x}\right)_z = \left(\frac{\partial \alpha}{\partial x}\right)_\zeta + \left(\frac{\partial \alpha}{\partial \zeta}\right)\left(\frac{\partial \zeta}{\partial x}\right)_z$$

$$\left(\frac{\partial \alpha}{\partial y}\right)_z = \left(\frac{\partial \alpha}{\partial y}\right)_\zeta + \left(\frac{\partial \alpha}{\partial \zeta}\right)\left(\frac{\partial \zeta}{\partial y}\right)_z$$

$$J \frac{\partial \alpha}{\partial z} = \frac{\partial \alpha}{\partial \zeta} \qquad \text{(B8)}$$

$$\left(\frac{\partial \zeta}{\partial x}\right)_z = M_x / J$$

$$\left(\frac{\partial \zeta}{\partial y}\right)_z = M_y / J$$

$$\frac{\tilde{d}}{dt} = \frac{\partial}{\partial t} + u \left(\frac{\partial}{\partial x}\right)_\zeta + v \left(\frac{\partial}{\partial y}\right)_\zeta + \omega \frac{\partial}{\partial \zeta}$$

where the definitions of J, M_x and M_y and the expression for the vertical velocity ω in the new system are

$$J \equiv \frac{\partial(x,y,z)}{\partial(x,y,\zeta)} = \frac{\partial z}{\partial \zeta}$$

$$M_x = -\left(\frac{\partial z}{\partial x}\right)_\zeta , \qquad M_y = -\left(\frac{\partial z}{\partial y}\right)_\zeta \qquad \text{(B9)}$$

$$w = J\omega + u\left(\frac{\partial z}{\partial x}\right)_\zeta + v\left(\frac{\partial z}{\partial y}\right)_\zeta \qquad \left(\omega = \frac{\tilde{d}\zeta}{dt}\right)$$

Here α stands for any one of the dependent or independent variables and the subscripts z and ζ for partial differentiation in the respective coordinate system. J is the Jacobian determinant of the mapping, also known as the stretching coefficient and M_x and M_y can be interpreted as the slopes in the ξ and η directions, respectively.

As to the shape of the new vertical coordinate $\zeta = \zeta(x,y,z)$, it seems natural to assume

$$\zeta = h \frac{z - z_s(x,y)}{h - z_s(x,y)} \tag{B10}$$

such that $\zeta = 0$ for $z = z_s(x,y)$ and $\zeta = h$ for $z = h$, where h is the height of the BL and $z_s(x,y)$ is the profile of the lower boundary. Solving B(10) for $z = z(x,y,\zeta)$, the expression for the reverse mapping is

$$z = z_s(x,y) + [1 - z_s(x,y)/h]\zeta \tag{B11}$$

However, in the present investigation, the simplifying approximation $z_s(x,y)/h \approx 0$ will be introduced. Therefore the expression for ζ from (B11) is simply,

$$\zeta = z - z_s(x,y), \tag{B12}$$

with the inverse mapping

$$z = z_s(x,y) + \zeta \tag{B13}$$

Thus by partial differentiation of (B13) the expressions for the slopes M_x and M_y, the Jacobian determinant and the vertical velocity for the total and deviation fields ω and ω' respectively in the new system are

$$M_x = -(\frac{\partial z}{\partial x})_\zeta = -\frac{\partial z_s}{\partial x} = \tan \psi_x > 0$$

$$M_y = -(\frac{\partial z}{\partial y})_\zeta = -\frac{\partial z_s}{\partial y} = \tan \psi_y > 0 \qquad \text{(B14)}$$

$$J \equiv 1 , \quad w = \omega - u \tan \psi_x - v \tan \psi_y$$

$$w' = \omega' - u' \tan \psi_x - v' \tan \psi_y$$

where the terrain profile $z_s(x,y)$ has been approximated by an inclined plane and therefore ψ_x and ψ_y are respectively the inclined plane angles in the ξ and η directions and are defined positive or negative if the axes are above or below the horizontal plane respectively (Fig. 1a). It can be seen that (B14) can also be obtained from (B11) by assuming the slopes M_x and M_y are independent of ζ and equal to their values at $\zeta = 0$.

Substituting (B8) into (B6) and then (B14) into the result, the expressions (B6) become

$$\frac{\tilde{du'}}{dt} - \tilde{f} v' = - (\frac{\partial \pi'}{\partial x})_\zeta - \beta\theta' \tan \psi_x + \frac{\partial}{\partial \zeta} (K \frac{\partial u'}{\partial \zeta})$$

$$\frac{\tilde{dv'}}{dt} + \tilde{f} u' = - (\frac{\partial \pi'}{\partial y})_\zeta - \beta\theta' \tan \psi_y + \frac{\partial}{\partial \zeta} (K \frac{\partial u'}{\partial \zeta}) \qquad \text{(B15)}$$

$$\frac{\tilde{d\theta'}}{dt} + (\omega' - u' \tan \psi_x - v' \tan \psi_y)\gamma = \frac{\partial}{\partial \zeta}(\alpha_H^o K \frac{\partial \theta'}{\partial \zeta})$$

$$(\frac{\partial u'}{\partial x})_\zeta + (\frac{\partial v'}{\partial y})_\zeta + \frac{\partial \omega'}{\partial \zeta} = 0$$

$$\frac{\partial \pi'}{\partial \zeta} = \beta\theta' \quad , \quad \beta = g/\theta_m$$

The assumption of horizontal homogeneity together with the lower

boundary condition $\omega' = 0$ at $\zeta = 0$ yields, from the continuity equation in (B15), $\omega' \equiv 0$ for all ζ . Hence with the assumptions of steady state in (B15), the following simple expressions for the BL above sloping surface are arrived at:

$$\begin{aligned} \frac{d}{d\zeta}(K \frac{du'}{d\zeta}) + \tilde{f} v' - \beta \theta' \tan \psi_x &= 0 \\ \frac{d}{d\zeta}(K \frac{dv'}{d\zeta}) - \tilde{f} u' - \beta \theta' \tan \psi_y &= 0 \qquad \text{(B16)} \\ \frac{d}{d\zeta}(K \frac{d\theta'}{d\zeta}) + (u' \tan \psi_x + v' \tan \psi_y)\gamma' &= 0 \quad , \quad \gamma' = \gamma/\alpha_H^o \end{aligned}$$

As to the derivation of the equations for the terrain slope angle and the direction of the fall-line vector (FLV), first it can be shown that the coordinate-transformation from a horizontal Cartesian system with coordinates, say, $X = (x,y,z)^T$ twisted an angle σ from the projection onto the horizontal plane of the fall-line vector (FLV), say, x" to the non-twisted and ψ-sloping Cartesian system, having the same origo, with coordinates, say, $X' = (x',y',\zeta)^T$ is

$$X' = \begin{pmatrix} \cos\psi \cos\sigma & \cos\psi \sin\sigma & -\sin\psi \\ -\sin\sigma & \cos\sigma & 0 \\ \sin\psi \cos\sigma & \sin\psi \sin\sigma & \cos\psi \end{pmatrix} \cdot X \ , \qquad \textit{(B17)}$$

where the x' axis is oriented positive downward along the FLV, σ is measured from x(-) to x"(-) in the horizontal plane and is positive in the counterclockwise sense and ψ is the terrain slope angle (defined always positive)(Fig. 1a). (B17) shows that the relative orientation of any two Cartesian systems such as X and X' with common origo can be expressed in terms of σ and ψ. From (B17), a two-dimensional coordi-

nate transformation from a σ-twisted Cartesian system with coordinates, say, $H = (\xi,\eta)^T$ to the non-twisted Cartesian system with coordinates, say, $X' = (x',y')^T$ is obtained by simply setting $\psi = 0$ in (B17). Thus

$$X' = \begin{pmatrix} \cos\sigma & \sin\sigma \\ -\sin\sigma & \cos\sigma \end{pmatrix} \cdot H \qquad \text{(B18)}$$

Note that the transformation matrices in (B17) and (B18) are orthogonal (i.e., the inverse matrix equals its transpose).

As illustrated in Fig. 1a, the σ-twisted horizontal system X is the system where (B1)-(B6) are originally written and the σ-twisted ψ-inclined system with coordinate, say, $\Pi = (\xi,\eta,\zeta)^T$ is the system where the Eqs. (B15) and (B16) are written. From Fig. 1a, it is also seen that the Π-system can be obtained by rotating in counterclockwise sense the X-system an angle ψ with the positive y′ as the axis of rotation and that the non-twisted ψ-inclined system X′ is the system where the final equations will appear.

Next, if (a,b,c) are the coordinates of a vector $\underline{V}$ in the X-system as shown in Fig. 1b, then

$$\sin\psi_V = \frac{c}{(a^2 + b^2 + c^2)^{1/2}} \qquad \text{(B19)}$$

For $\underline{V}$ equal to $\underline{V}_\xi$ or $\underline{V}_\eta$ (see Fig. 1a) with coordinates $(-\cos\sigma,\sin\sigma,0)^T$ or $(\sin\sigma,\cos\sigma,0)^T$ respectively in the X′-system, it follows from the inverse of (B17) that the coordinates a, b and c for $\underline{V}_\xi$ and $\underline{V}_\eta$ in the X-system are respectively,

$$
\begin{aligned}
(a,b,c) &= [-\cos\psi\cos^2\sigma - \sin^2\sigma, \\
&\qquad (1-\cos\psi)\sin\sigma\cos\sigma, \ \sin\psi\cos\sigma] \\
(a,b,c) &= [(1-\cos\psi)\sin\sigma\cos\sigma, \\
&\qquad (\cos\psi\sin\sigma + \cos\sigma)\sin\sigma, \ -\sin\psi\sin\sigma]
\end{aligned}
\tag{B20}
$$

From (B20) and (B19), it follows that

$$
\begin{aligned}
\sin\psi_x &= \sin\psi\cos\sigma \\
\sin\psi_y &= -\sin\psi\sin\sigma
\end{aligned}
\tag{B21}
$$

A geometrical visualization of (B19) - (B21) and the meaning of the angles σ, ψ_x, ψ_y and ψ are given in Fig. 1 and (B20) can be considered to be a system of two equations for the two unknowns ψ and σ, i.e., the maximum slope angle (along the FLV) and the direction of the FLV if the slopes in <u>any</u> two perpendicular directions ψ_x and ψ_y are known. Alternatively, ψ and σ can be computed from either one of the expressions in (B20) if the slopes, say, ψ_1 and ψ_2 of two arbitrary traverses in the directions, say, θ_1 and θ_2 from a fixed reference point are known. This latter approach has been used, e.g. by Dalrymple et al. (1963) to calculate ψ and σ of the South Pole.

From (B16) and (B18), the following form of the final equations in the X'-system derived in GM is obtained:

$$
\begin{aligned}
\frac{d}{d\zeta}\left(K\frac{du''}{d\zeta}\right) - \tilde{f}\,v'' - \beta\,\psi\,\theta' &= 0 \\
\frac{d}{d\zeta}\left(K\frac{dv''}{d\zeta}\right) + \tilde{f}\,u'' &= 0 \\
\frac{d}{d\zeta}\left(K\frac{d\theta'}{d\zeta}\right) + \gamma'\,\psi\,u'' &= 0
\end{aligned}
\tag{B22}
$$

where

$$u'' = u'\cos\sigma + v'\sin\sigma$$
$$v'' = v'\cos\sigma - u'\sin\sigma \qquad \text{(B23)}$$

and

$$\psi = (\psi_x^2 + \psi_y^2)^{1/2} \ , \ \sin\sigma = \psi_y/\psi \ , \ \cos\sigma = \psi_x/\psi$$
$$G = (U^2 + V^2)^{1/2} \qquad \text{(B24)}$$

Note that in (B22) and (B24) because of the smallness of the angles ψ_x, ψ_y and ψ the approximations tan x = sin x = x and cos x = 1 are used for x either ψ_x, ψ_y or ψ. Furthermore, as already mentioned above in deriving (B22), the positive x'-axis is made to coincide with the FLV (see Fig. 1a) and the meaning of the geostrophic wind $\underline{G}$ and its direction χ from the FLV is given in Fig. 2.

It is interesting to note that (B22) is a generalization of the usual Ekman BL equations to include the terms containing ψ, of the Prandtl slope wind equations to include the terms containing $\tilde{f}$ and G in u" and v", of Gutman and Malbakhov's (1964) equations to include G in u" and v", and of Brost and Wyngaard's equations to include the term containing γ. Moreover, it is interesting to note that (B22) is one of the few examples of linear coupling between the wind and temperature fields in the atmosphere.

Eqs. (B22) can be compressed further by the following linear combination

$$\frac{d}{d\zeta}\left(K \frac{dp}{d\zeta}\right) - i \frac{\tilde{f}}{a} p = 0$$
$$\frac{d}{d\zeta}\left(K \frac{dq}{d\zeta}\right) = 0 \qquad \text{(B25)}$$

where

$$p = a\,(v'' - b\beta\psi\theta'/f) - ibu''$$
$$q = v'' + bf\theta'/(\gamma'\psi) \tag{B26}$$

and

$$a = [1 + (N\psi/f)^2]^{-1/2} \quad , \quad N = (\gamma'\beta)^{1/2}$$
$$\tilde{f} = 2\Omega\sin\phi \qquad (f = |\tilde{f}|) \tag{B27}$$
$$b = \operatorname{sign}\phi = \begin{cases} +1 \text{ for } \phi \geq 0 \\ -1 \text{ for } \phi < 0 \end{cases}$$

The parameter b in (B27) is introduced to make (B25) applicable for either Northern or Southern Hemispheres.

From the first equation in (B25), in analogy with the Ekman BL equations, the characteristic length scale for the BL above sloping terrain must be

$$\lambda_s = \frac{ku_*}{(f/a)} = \frac{aku_*}{f} \tag{B28}$$

where

$$u_* = (\tau/\rho_o)^{1/2} \quad , \quad T_* = -H/(k\rho_o c_p u_*) \tag{B29}$$

If the following definitions for non-dimensional variables (denoted by bars)

$$\zeta = \lambda_s\bar{\zeta} \quad ; \quad p = \frac{u_*}{k}\bar{p} \quad ; \quad q = \frac{u_*}{k}\bar{q}$$
$$K = ku_*\lambda_s\bar{K} \quad , \quad h = \lambda_s\bar{h} \quad , \quad z_o = \lambda_s\bar{z}_o \tag{B30}$$

are substituted into (B25), its non-dimensional form reads,

$$\frac{d}{d\bar{\zeta}}\left(\bar{K}\frac{d\bar{p}}{d\bar{\zeta}}\right) - i\,\bar{p} = 0$$

$$\frac{d}{d\bar{\zeta}}\left(\bar{K}\frac{d\bar{q}}{d\bar{\zeta}}\right) = 0 \qquad \text{(B31)}$$

where

$$\bar{p} = a(kv''/u_* - b\mu\,\frac{\psi}{k^2}\,\frac{\theta'}{T_*}) - i\,b(ku''/u_*)$$

$$\bar{q} = (kv''/u_*) + b\left(\frac{a^2}{1-a^2}\right)\mu\,\frac{\psi}{\kappa^2}\,\frac{\theta'}{T_*} \qquad \text{(B32)}$$

$$\mu = k^3\,\beta\,T_*/(f\,u_*)$$

Finally Eqs. (1) and (2) of the main text are obtained from (B31) with ζ replaced by z and with the overbars in K, p and q omitted for simplicity.

APPENDIX C

The Generating Function R for R_n in (4.8)

R is the generating function for R_n, i.e.,

$$R(\Delta) = \sum_{n=-1}^{\infty} R_n \Delta^n$$

where Δ is an independent variable and

$$R(\Delta) = z_0 F G^{n-\theta_1} \qquad (z_0 \text{ is } z_n \text{ for } n = 0)$$

$$F = \sum_{n=0}^{\infty} s_n \Delta$$

$$G = \sum_{m=0}^{\infty} \{ \sum_{n=2}^{\infty} y_n \Delta^{n-\theta_1} \}^m$$

$$s_n = q_n \sum_{j=0}^{[n/2]} \{S + 2[n - \theta_3 - (2 + S)j]\phi_j\} \frac{S^{n-2j}}{(n-2j)!(j!)^2}$$

$$y_n = z_n \sum_{j=0}^{[n/2]} [n - \theta_3 - (2 + S)j] \frac{S^{n-2j}}{(n-2j)!(j!)^2}$$

$$\phi_j = \sum_{k=1}^{j} 1/k \quad ; \quad \phi_0 = 0$$

$$q_n = \begin{cases} 1 & , \ n \text{ even} \\ Q & , \ n \text{ odd} \end{cases}$$

$$z_n = \begin{cases} \theta_3 - \theta_1 T & , \ n \text{ even} \\ \theta_3 Q - \theta_1 & , \ n \text{ odd} \end{cases}$$

$T = \tanh(a)$

$Q = \coth(a)$

$[n/2]$ = greatest integer $\leq n/2$

and

unstable ($\mu_s < 0$)	stable ($\mu_s > 0$)
$\theta_1 = 0$	$\theta_1 = 1$
$\theta_3 = 1$	$\theta_3 = 0$
$S = 3$	$S = 1$
$a = -(i\ 9\sigma)^{1/2}$	$a = -(i\ \sigma)^{1/2}$

APPENDIX D

Solution of the integral equation (4.14)

It can be seen that the integral

$$I = \int \frac{\sum_{k=0}^{M} a_k z^k}{a z^{\alpha} + b z^{\beta}} dz \qquad (D1)$$

where a, b and $\{a_k\}_{k=0}^{M}$ are complex numbers ($a,b \neq 0$), and α and β are rational numbers ($\alpha \neq \beta$), has the following solution:

$$I = \ell \sum_{k=0}^{M} (\sigma_k a_k / c_k)\{(t_k^{m_k/n}/n) \sum_{\lambda=1}^{n} w_\lambda^{m_k} \ell n(z^{-\sigma_k/\ell} - t_k^{1/n} w_\lambda) - \qquad (D2)$$

$$- \sum_{\lambda=1}^{N_k} (-1)^{\lambda} t_k^{\lambda} \cdot z^{\sigma_k(\lambda n - m_k)/\ell} / (\lambda n - m_k)\} + \text{constant}$$

In (D2) the various symbols have the following meaning:

$$\left.\begin{aligned} \alpha &= n_\alpha/m_\alpha \\ \beta &= n_\beta/m_\beta \end{aligned}\right\} n_\alpha, m_\alpha, n_\beta, m_\beta \text{ are integers}$$

$$\ell = |\text{LCM}(m_\alpha, m_\beta)|, \text{ (LCM = Least Common Multiple)} \qquad (D3)$$

$$\varepsilon = \beta - \alpha$$

$$n = \ell\,|\varepsilon|, \text{ (integer)}$$

$$\sigma_k = \text{sign}\,[(\alpha + \beta - |\varepsilon|)/2 - k - 1], \quad [\text{sign}(0) = 1]$$

$$m_k = \ell\, \lfloor (\alpha + \beta + \sigma_k |\varepsilon|)/2 - k - 1 \rfloor, \quad \text{(integer)}$$

$$N_k = \text{entier}\,[(m_k - 1)/n] \quad [\text{greatest integer} \leq (m_k - 1)/n]$$

$$c_k = [1 + \text{sign}(-\sigma_k \varepsilon)]\, a/2 + [1 + \text{sign}(\sigma_k \varepsilon)]\, b/2 \qquad \text{(D3)}$$

$$t_k = (b/a)^{\text{sign}(\sigma_k \varepsilon)}$$

$$\omega_\lambda = e^{i(2\lambda - 1)\pi/n}$$

$\ell n(x+iy) = (1/2)\, \ell n(x^2 + y^2) + i\, \arg(x,y)$, $(x,y = \text{real})$ and arg is defined in (3.15).

REFERENCES

Arya, S.P.S., 1975. Geostrophic drag and heat transfer relations for the atmospheric boundary layer. Quart. J. Roy. Meteor. Soc., 101, 147-161.

Ball, F.K., 1960. Winds on the ice slopes of Antarctica. Proceedings of the symposium on Antarctic Meteorology held in Melbourne, February 1959, Pergamon Press, 9-16.

Behrendt, J.C., 1967. Gravity increase at the South Pole. Science, 155, 1015-1016.

Bentley, Ch., 1971. Secular increase of gravity at South Pole Station. Antarctic Snow and Ice Studies II, Antarctic Research Series, 16, 191-198.

Brost, R.A., and J.G. Wyngaard, 1978. A model study of the stably stratified planetary boundary layer, J. Atmos. Sci., 35, 1427-1440.

Businger, J.A., J.C. Wyngaard, Y. Izumi and E.F. Baradley, 1971. Flux-profile relationships in the atmospheric surface layer. J. Atmos. Sci., 28, 181-189.

Charney, J., 1969. What determines the thickness of the planetary boundary layer in a neutrally stratified atmosphere? Okeanologia, 9, 111-113.

Dalrymple, P.C., H.H. Lettau, and S.H. Wollaston, 1966. South Pole micro-meteorology program, Part II: Data analysis. Studies in Antarctic Meteorology, Research Series, 9, 13-57.

Deacon, E.L., 1973. Geostrophic Drag Coefficients. Boundary-Layer Meteorology, 5, 321-340.

Drewry, D.J. (Ed.), 1983. The surface of the Antarctic Ice Sheet.

Sheet 2 of Antarctica. Glaciological and Geophysical Folio. Scott Polar Research Institute, Univ. of Cambridge, U.K.

Gutman, L.N., 1969. Introduction to the Nonlinear Theory of-Mesoscale Meteorological Processes, (Ed. G. I. Marchuk) Gidrometeor Izdatal'stvo, Leningrad. [Translated from Russian by Israel Program for Scientific Translations, Jerusalem 1972, 224 pp.]

Gutman, L.N., and V.M. Malbakhov, 1964. On the theory of Katabatic winds of Antarctic. Meteorologicheskiye Issledovaniye No. 9 English translation by U. Radok available at the Department of Meteorology, University of Melbourne, Australia.

Gutman, L.N., and J.W. Melgarejo, 1981. On the laws of geostrophic drag and heat transfer over a slightly inclined terrain. J. Atmos. Sci., 38, 1714-1724.

Kazakov, A.L. and G.L. Lazriev, 1978. Parameterization of the atmospheric surface layer and of the active soil layer. Izv., Atmos. Oceanic Phys., 14, 186-191.

Kazanski, A.B., and A.S. Monin, 1961. On the dynamic interaction between the atmosphere and the earth's surface. Izv., Atmos. Oceanic Phys., 5, 514-515.

Kuhn, M., H.H. Lettau and A.J. Riordan, 1977. Stability-related wind spiraling in the lowest 32 meters. Meteorological Studies of Plateau Station, Antarctica, Antarctic Res. Ser., 25, 93-111.

Laikhtman, D.L. and Ye V. Kurdova, 1980. A model of the planetary boundary layer, Izv., Atmos. Oceanic Phys., 6, 483-488.

Laikhtman, D.L., and D.L. Yordanov, 1979. On the vertical velocity at the top of the planetary boundary layer in nonstationary conditions. Bound.-Layer Meteor., 17, 293-296.

Lettau, H.H., 1966. A case study of Katabatik flow on the south polar

plateau. Studies in Antarctic Meteorology, Antarctic Research Series, 9, 1-11.

Lettau, H.H., and W. Schwerdtfeger, 1967. Dynamics of the surface-wind regime over the interior of Antarctica: Antarctic Journal of the U.S., 2(5), 155-158.

Louis, J.F., M. Tiedtke and J.F. Geleyn, 1981. A short history of the operational PBL parameterization at ECMWF, Workshop on Planetary Boundary Layer Parameterization, European Center for Medium Range Weather Forecasts, Reading, England, 59-80.

Monin, A.S., 1986. An Introduction to the Theory of Climate. Dordrecht Holland: D. Reidel Publ. Comp., 261 pp.

Melgarejo, J.W., and J.W. Deardorff, 1974. Stability Functions for the Boundary-layer resistance laws based upon observed Boundary-layer heights. J. Atmos. Sci., 31, 1324-1333.

McInnes, B., and U. Radok, 1984. Estimated Ages and Temperatures of South Pole ice. Antarctic Journal of the U.S., 19, 10-12

Neff, W.D., 1981. An observational and numerical study of the atmospheric boundary layer overlying the East Antarctic Ice Sheet. NOAA Technical Memorandum, ERL WPL-67. Wave Propagation Laboratory, Boulder, Colorado, 272 pp.

Panofsky, H.A., and J.A. Dutton, 1984. Atmospheric Turbulence, Models and Methods for Engineering Applications. John Wiley and Sons, New York, 397 pp.

Prandtl, L., 1942. Essentials of Fluid Dynamics, with applications to Hydraulics, Aeronautics, Meteorology and other Subjects. Authorized Translation. Hofner Publishing Company, 422-425.

Radok, U., 1981. The lower atmosphere of the polar regions. Sonderdruck aus der Geologischen Rundschau, 70, 703-724

Radok, U., 1983. Surface air flow at the South Pole. Unpublished manuscript, available from the author. Univ. of Colorado, CIRES, Campus Box 449, Boulder, Colorado 80309.

Schwerdtfeger, W., 1972. The vertical variation of the wind through the friction-layer over the Greenland ice cap. Tellus, 24, 13-16.

Schwerdtfeger, W. and M. Sponholz, 1970. Theory and observations of the wind in the friction layer over the Antarctic Plateau. Antarctic Journal of the U.S., 5, 175-176.

Watson, G.N., 1944. A Treatise on the Theory of Bessel Functions. Second Edition. Cambridge University Press, London: Bently House, 804 pp.

Wippermann, F., 1973. The Planetary Boundary-Layer of the Atmosphere. Annalen der Meteorologie (Neue Folge), 7, Deutscher Wetterdienst, Offenbach, a. M., 346 pp.

Zilitinkevich, S.S., 1972. Asymptotic expressions for the thickness of the Ekman layer, Izv. Atmospheric Oceanic Physics, 8, 1086-1090.

Zilitinkevich, S.S., D.L. Laikhtman and A.S. Monin, 1967. Dynamics of the atmospheric boundary layer, a Review, Izv. Atmos. Oceanic Phys., 3, 170-191.

Zilitinkevich, S.S., and A.S. Monin, 1974. Similarity theory for the planetary boundary layer of the atmosphere. Izv. Atmos. Oceanic Phys., 10, 353-359.

TABLE 1

The Universal Constants A, B and C for neutral stratification

($\mu_s = 0$)

Source[a]	A(0)	B(0)	C(0)
This investigation[b,c]	1.42	1.90	2.44(2.05)
This investigation[b,c] Eqs.(4.24)-(4.26)	1.57	2.55	1.32(-17.54)
Arya (1975)	5.14	1.01	1.86
Blackadar (1962)	6.7	1.8	
Blackadar and Tennekes (1968)	4.5	0.0	
Blinova and Kibel (1937)[b]	1.57	2.99	
Bobyleva et al. (1965)[b]	2.0	2.2	
Clarke (1970)	4.5	0.9	
Deacon (1973)	4.3	2.0	
Gill (1967)	4.6	1.7	
Johnson (1965)	4.7	2.3	
Lettau (1959)	4.8	2.8	
Lettau (1962)	4.65	1.1	
Kazanski and Monin (1961)[b]	1.69	2.49	
	1.81	1.7	
Yamamoto et al. (1968)	1.6	2.3	
Wippermann (1973)[b]	4.6	0.9	
Monin (1986)	4.3	1.1	

---

[a] The additional references can be found in either Deacon (1973), Wippermann (1973) or Zilitinkevich et al. (1967).

[b] The indicated values of A, B and C are from theory.

[c] The first value of C(0) is for r = 1 and the value in parenthesis is for r = 0 in (4.21).

TABLE II

Frequency distribution of cross-isobaric inflow angle (α) versus geostrophic wind direction (χ) from the fall-line vector directed towards 240° from North (or Greenwich meridian), i.e. towards approximately WSW. δ is the direction of the surface wind from the fall-line vector. All angles use counterclockwise turning as positive (adapted from Dalrymple et al., 1966, Table 5).

	χ (deg)															
$\alpha=\chi-\delta$ (deg)	15	38	60	83	105	128	150	173	195	218	240	263	285	308	330	353
405															2	3
382															1	3
360														1	1	
337														1		
315											1		1	1		
292												1	1		1	
270														1		
247									1		1					
225									1							
202									1							
180								1	2							
157							2	1	4	1						
135						1	3		5							
112					4	2	2	4	1							
90		1	2	3	9	14	9	1	1		1					
67	6	10	14	13	26	13	2		1							
45	9	9	19	29	8											
22	1	3	8	2			1			1						
0		1														
Total no of cases	16	24	43	47	47	30	19	7	17	2	3	1	2	4	5	6
%	5.9	8.8	15.7	17.2	17.2	11.0	7.0	2.6	6.2	0.7	1.1	0.4	0.7	1.5	1.8	2.2

Total cases = 273

Table III

Direction (from the fall-line vector) of the surface wind δ (when $\psi \ll f/N$, therefore $a = 1$) and the cross-isobaric inflow angle[a] α (when $\psi \equiv 0$) for $\mu_s = \pm \infty$ in the Southern Hemisphere ($\phi < 0$).

	$\delta_{+\infty}$		$\delta_{-\infty}$		$\alpha_{+\infty}$	$\alpha_{-\infty}$
σ \ r	0	1	0	1	any r	any r
0.1	273.82	273.76	121.76	118.25	1.91	complex
1	306.67	302.72	194.11	177.54	17.96	complex
10	50.65	14.68	217.83	193.33	46.27	complex
100	80.65	37.02	222.90	194.48	45.00	complex
1000	87.32	45.63	224.35	194.55	45.00	complex
∞	non-existant	50.69	225.00	194.55	45.00	complex

[a] These angles are positive because the computations are for the Southern Hemisphere.

a.

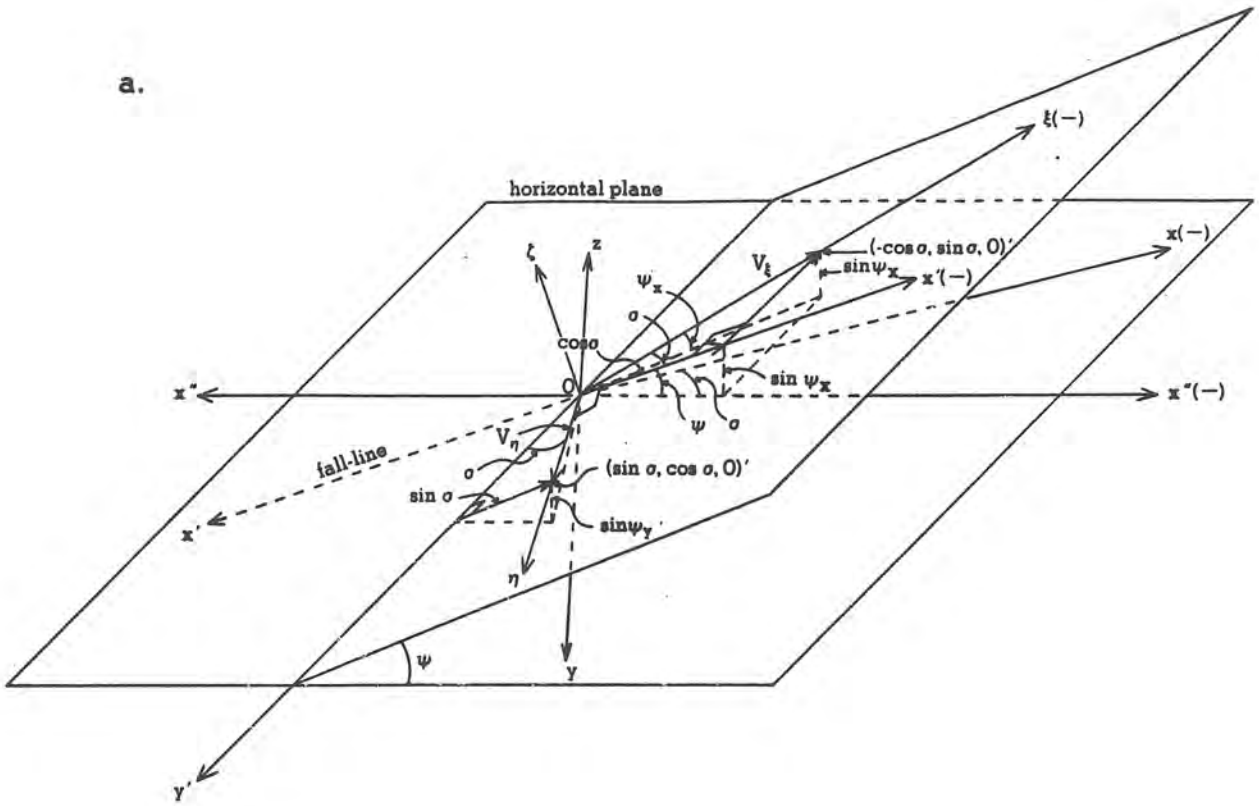

b.

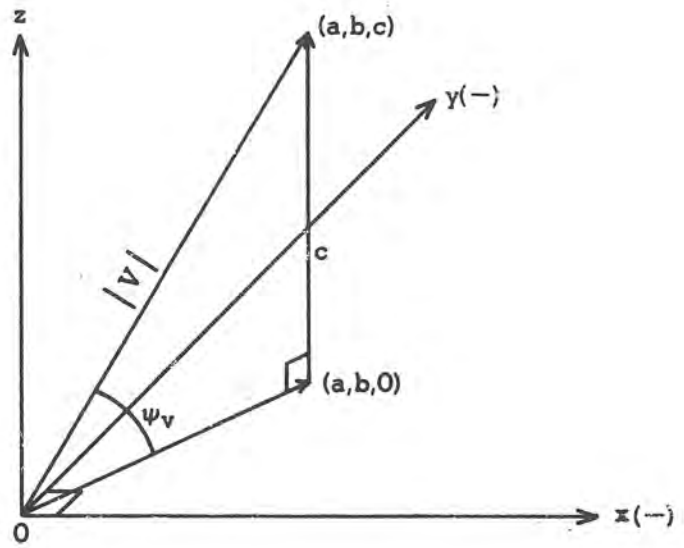

FIGURE 1. a) sketch of the Cartesian systems and of their transformation relations used in developing Eqs. (2.1) and (2.2). The σ-twisted system with coordinates $X = (x,y,z)^T$ is in the horizontal plane. The σ-twisted and non-twisted systems with coordinates $\Pi = (\xi, \eta, \zeta)$ and $X' = (x', y', \zeta)$ respectively, are in the ψ-sloping plane; b) sketch to help visualize Eqs. (B20) and (B21).

a.

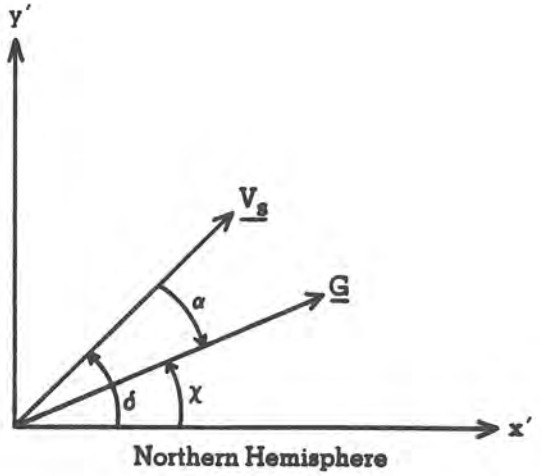

b.

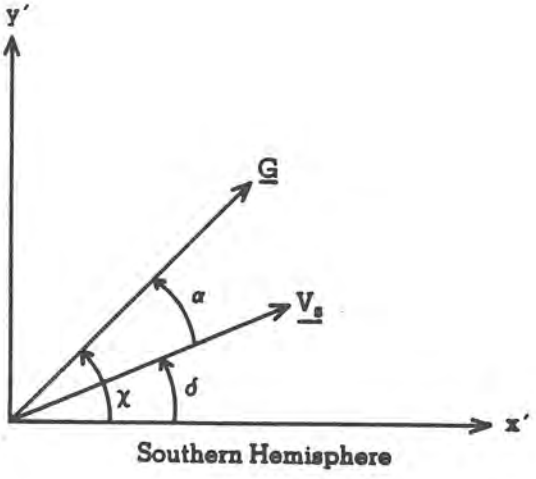

FIGURE 2. Sense of the angles α, δ and χ in the ψ-sloping (x',y')-plane, a) in the Northern Hemisphere and b) in the Southern Hemisphere. α = χ - δ is negative in the Northern Hemisphere and positive in the Southern Hemisphere.

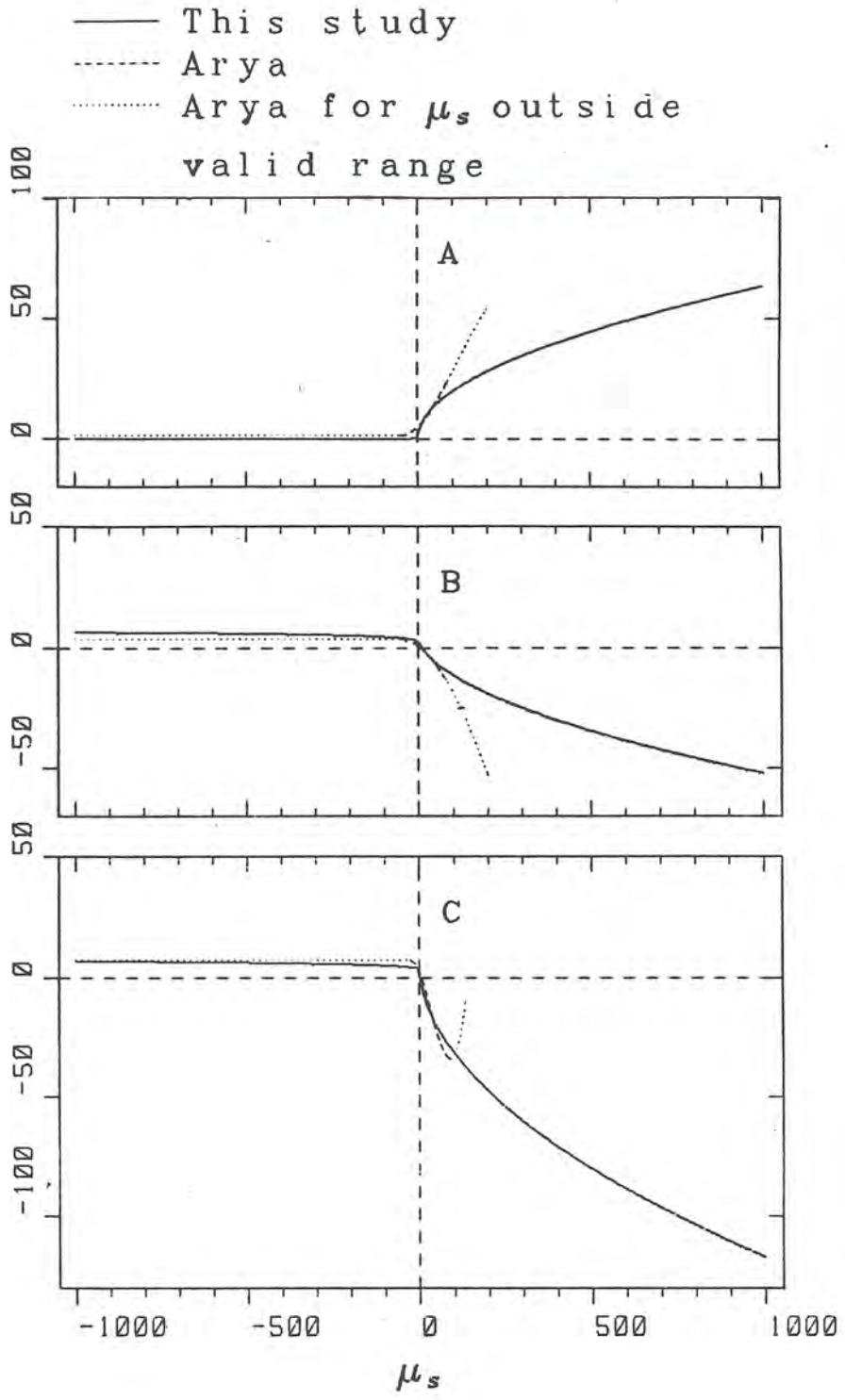

FIGURE 3. The universal functions A, B and C versus μ_s. The curves denoted by solid lines correspond to the results of this investigation and those denoted by dashed lines to the functions derived from observations by Araya (1975). The dotted portion of the dashed lines is where Araya's functions cease to be useful.

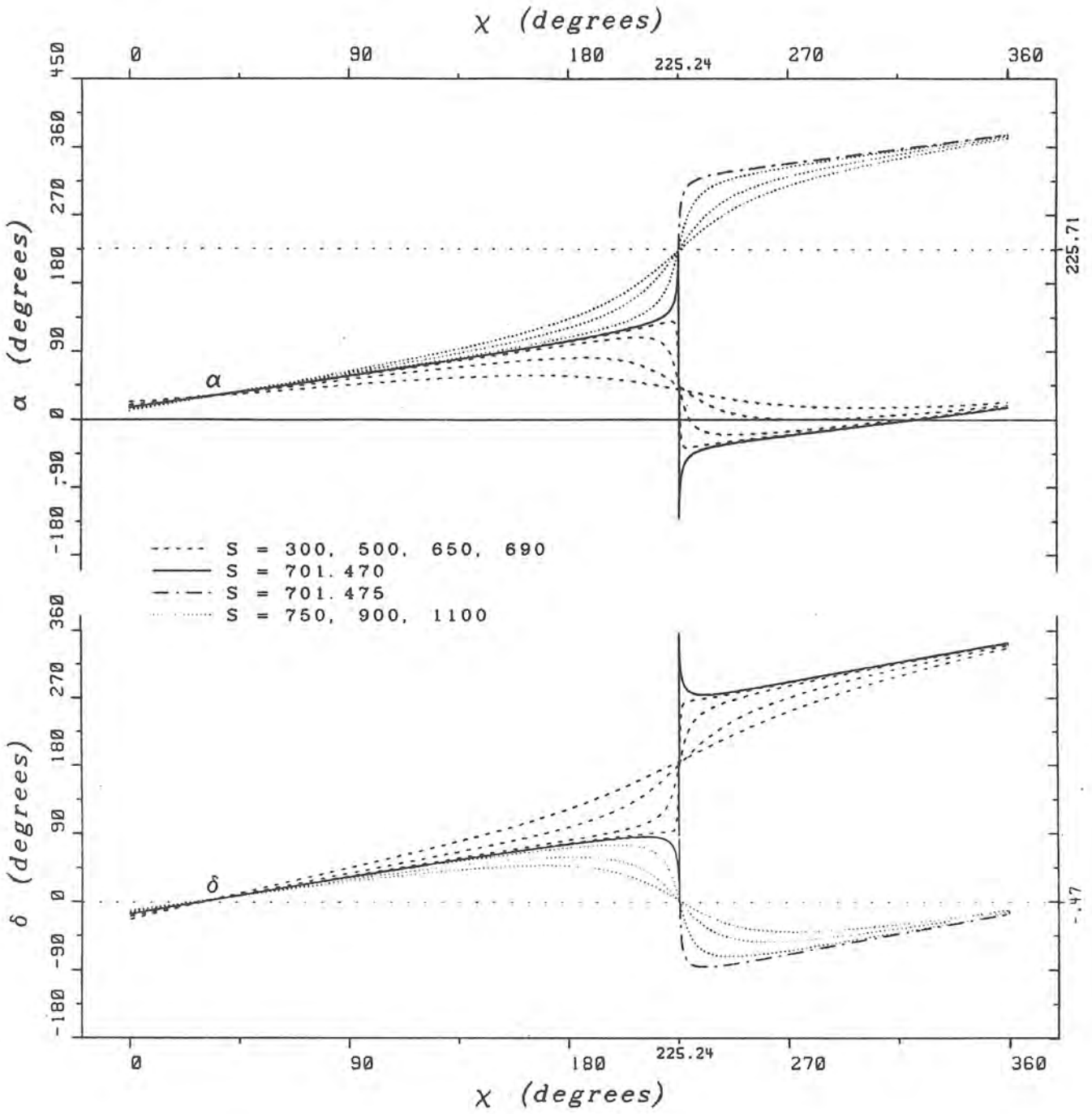

FIGURE 4. The cross-isobaric inflow angle α and the angle the surface wind ($\underline{V}_S$) makes with the fall-line vector δ versus the direction of the geostrophic wind ($\underline{G}$) from the fall-line vector χ for $\psi = 2 \times 10^{-3}$ rad, $R_0 = 10^7$ and for three different values of S: a) the 'oscillatory' regime for $S < S_c$, b) the 'transition' regime for $S = S_c$ (either of the 'oscillatory transition' type $S = S_{c^-}$ or of the 'staircase transition' type $S = S_{c^+}$) and c) the 'staircase' regime for $S > S_c$.

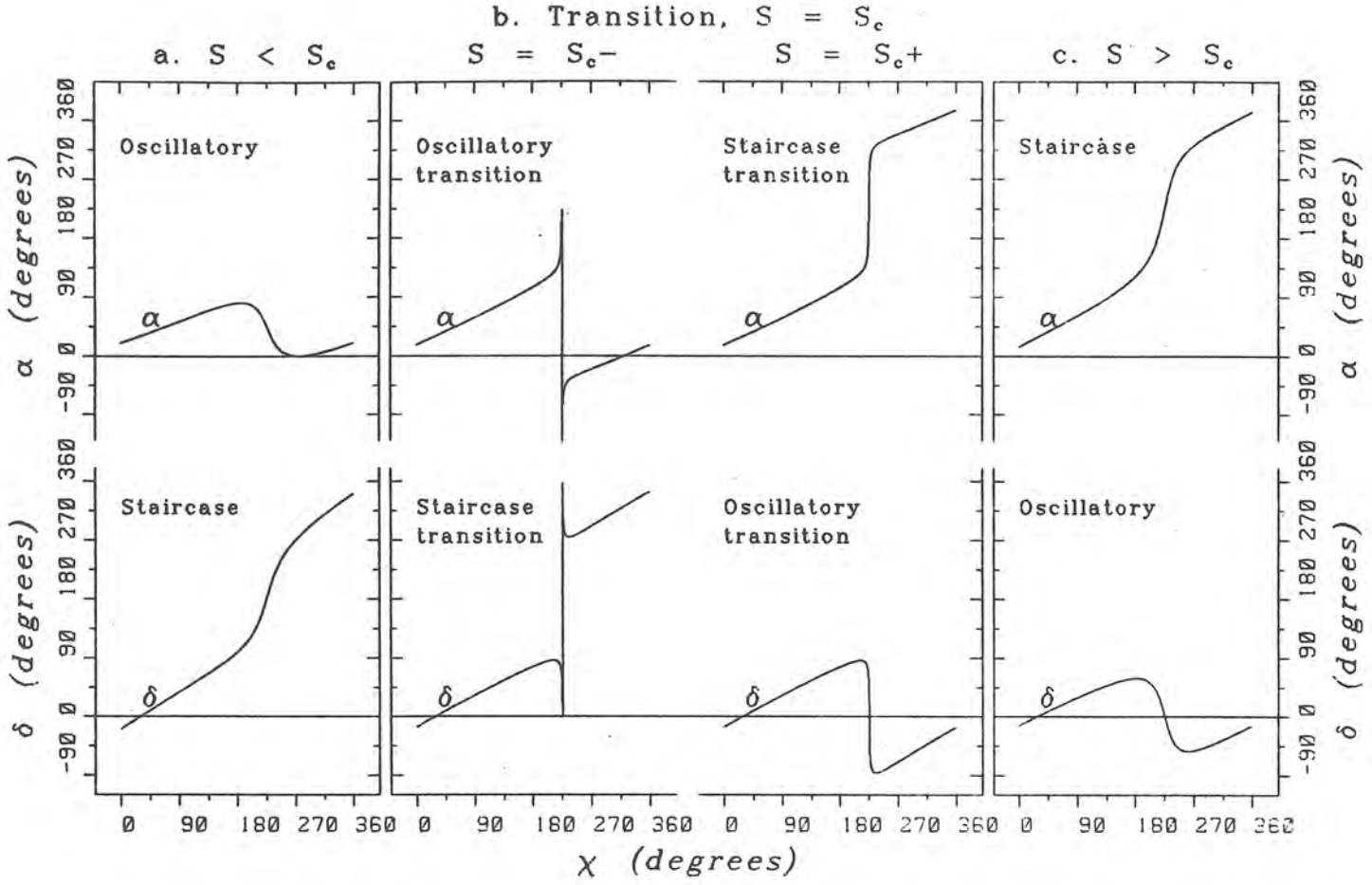

FIGURE 5. Diagrams of α and δ versus χ in all three regimes for the same values of ψ and R_0 as in Figure 4, except for S varying from 300 to 1100. The critical value S_c lies between S_c^- = 701.470 and S_c^+ = 701.475.

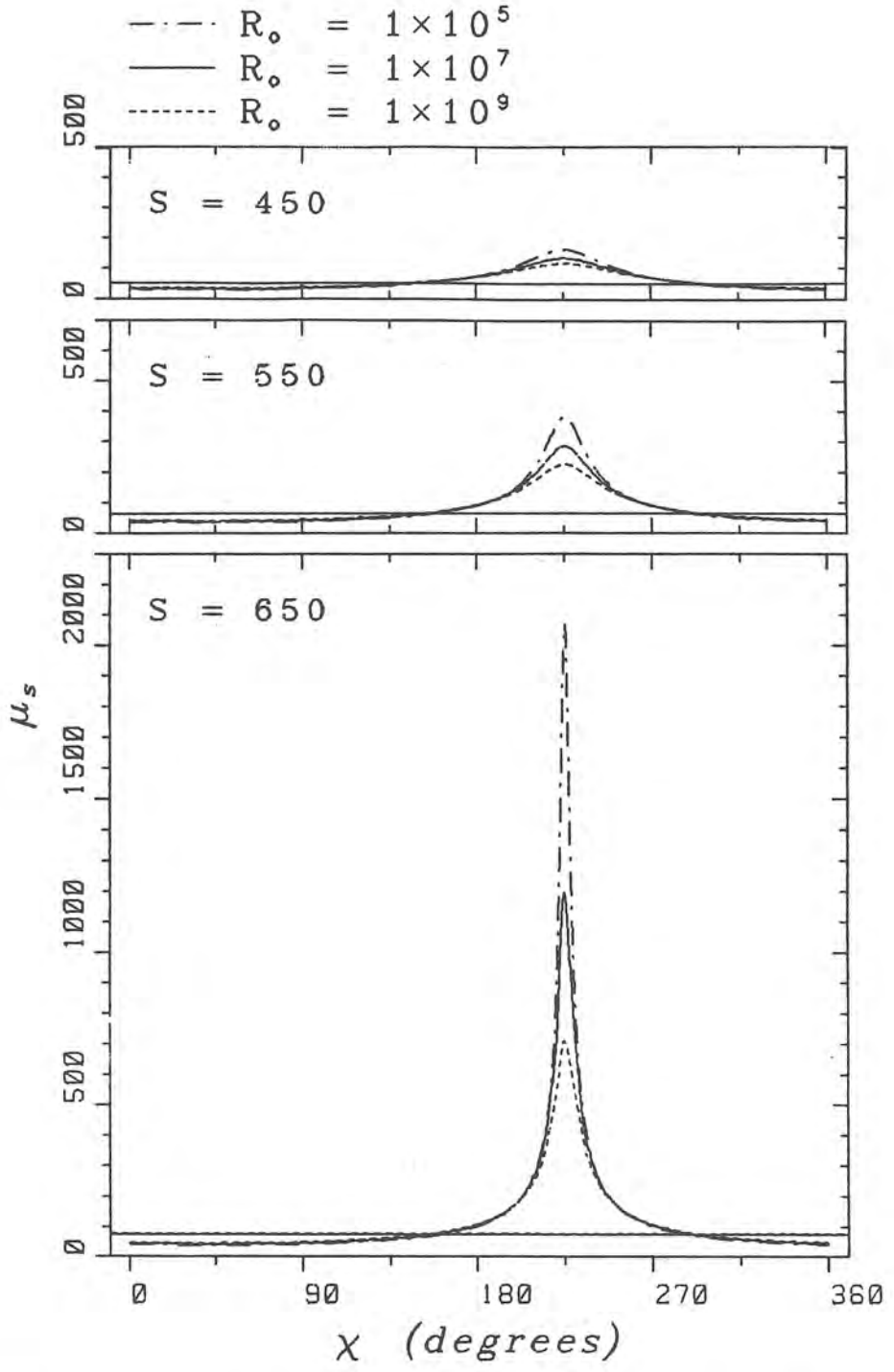

FIGURE 6. Internal stability μ_S versus χ for the 'oscillatory' regime, for $\psi = 2 \times 10^{-3}$ rad and for three values of S and R_0 as indicated in the figure. The horizontal solid lines represent the corresponding solutions for the case when the underlying surface is horizontal ($\psi=0$).

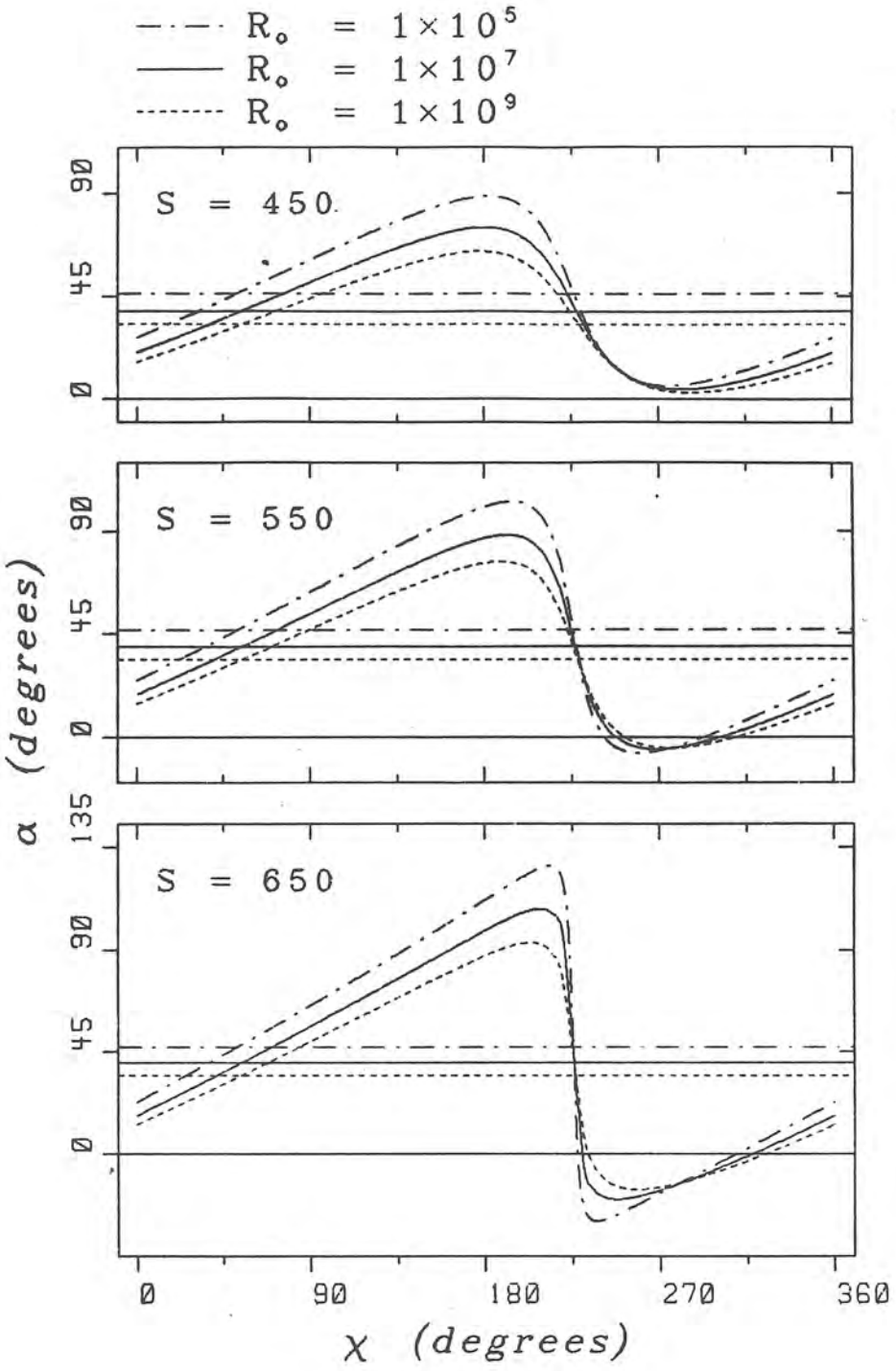

FIGURE 7. The same as Figure 6 except for α.

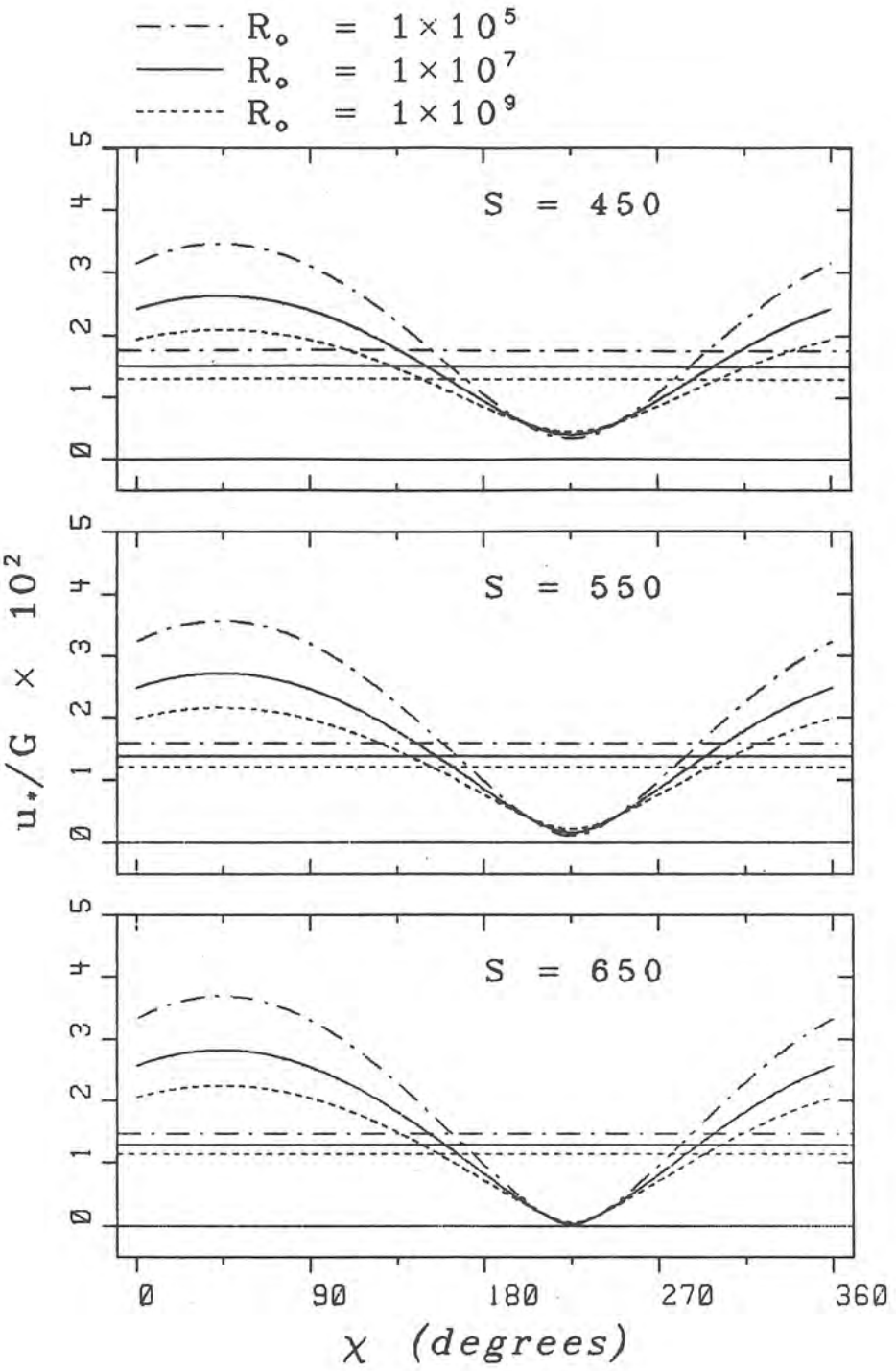

FIGURE 8. The same as Figure 6 except for u_*/G.

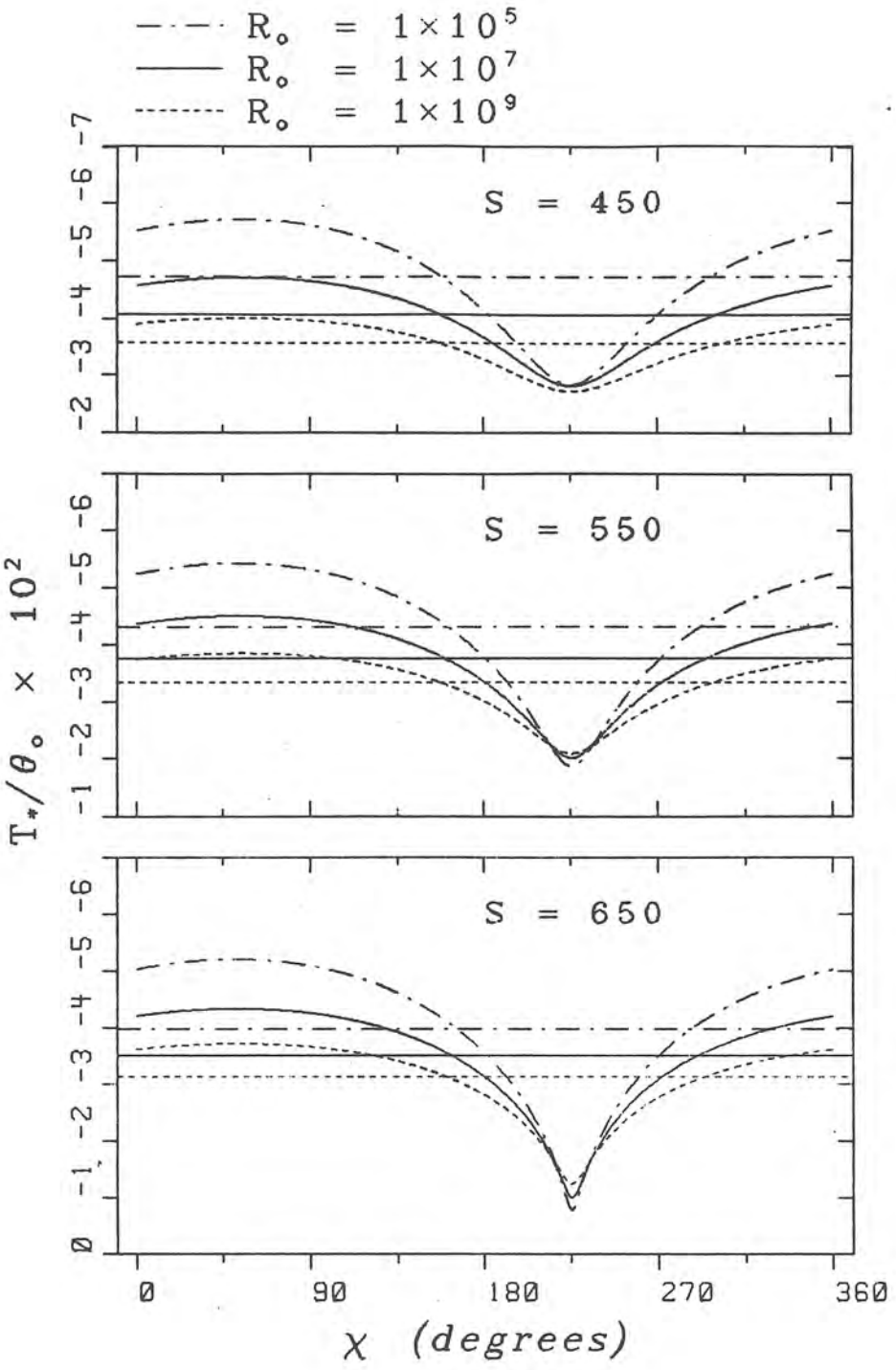

FIGURE 9. The same as Figure 6 except for T_*/Θ_0.

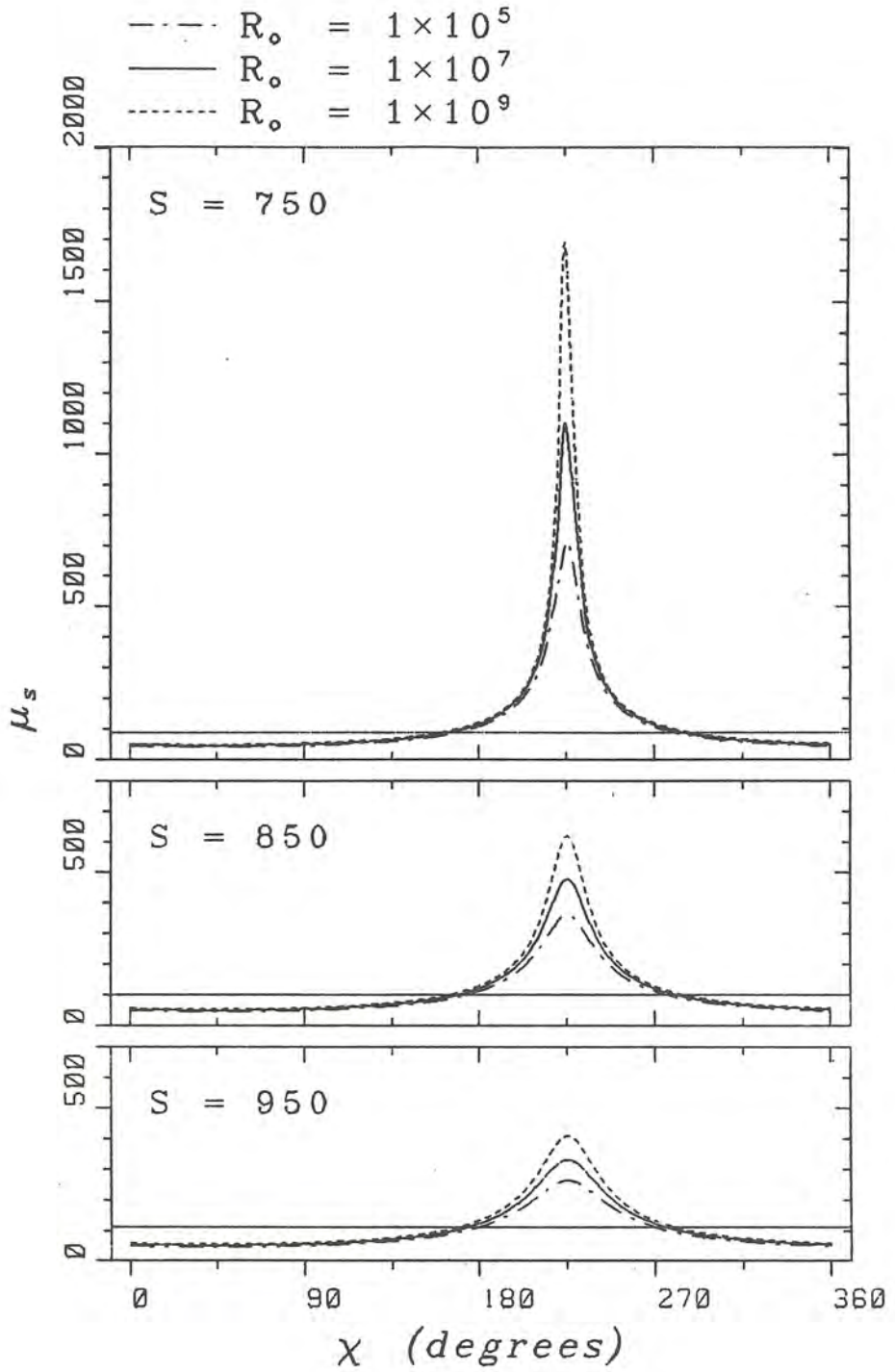

FIGURE 10. The same as Figure 6 except for the 'staircase' regime.

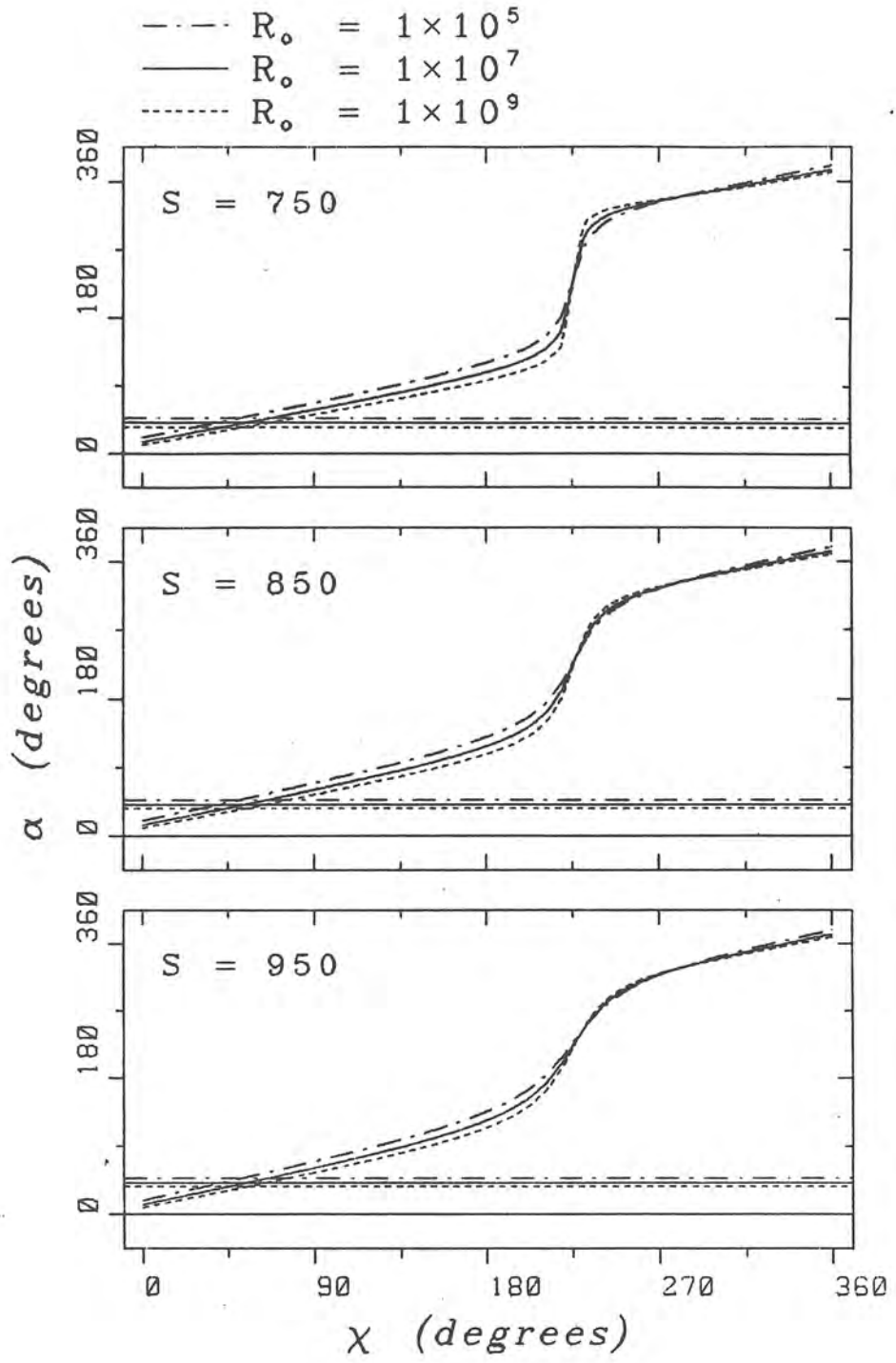

FIGURE 11. The same as Figure 7 except for the 'staircase' regime.

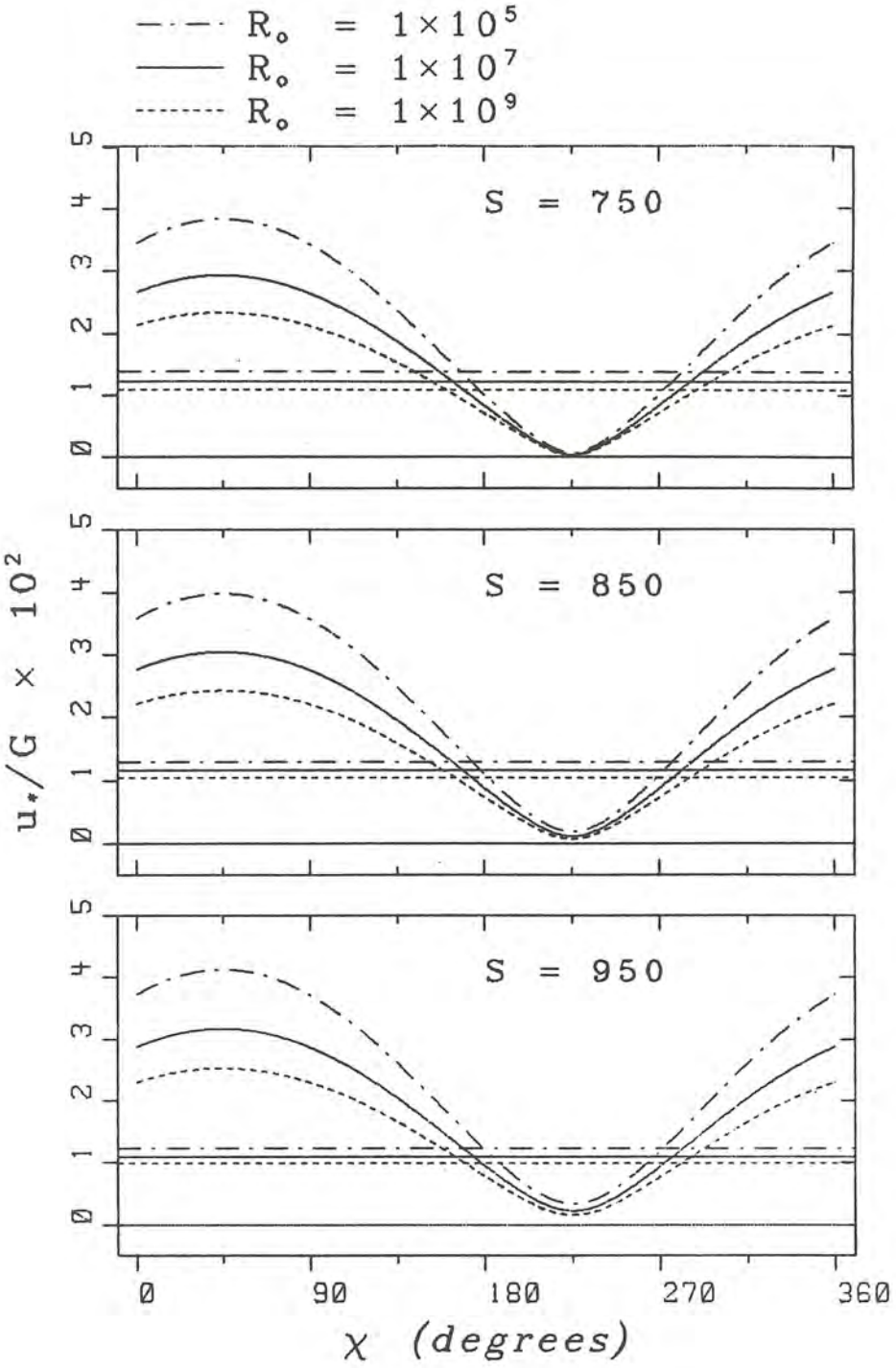

FIGURE 12. The same as Figure 8 except for the 'staircase' regime.

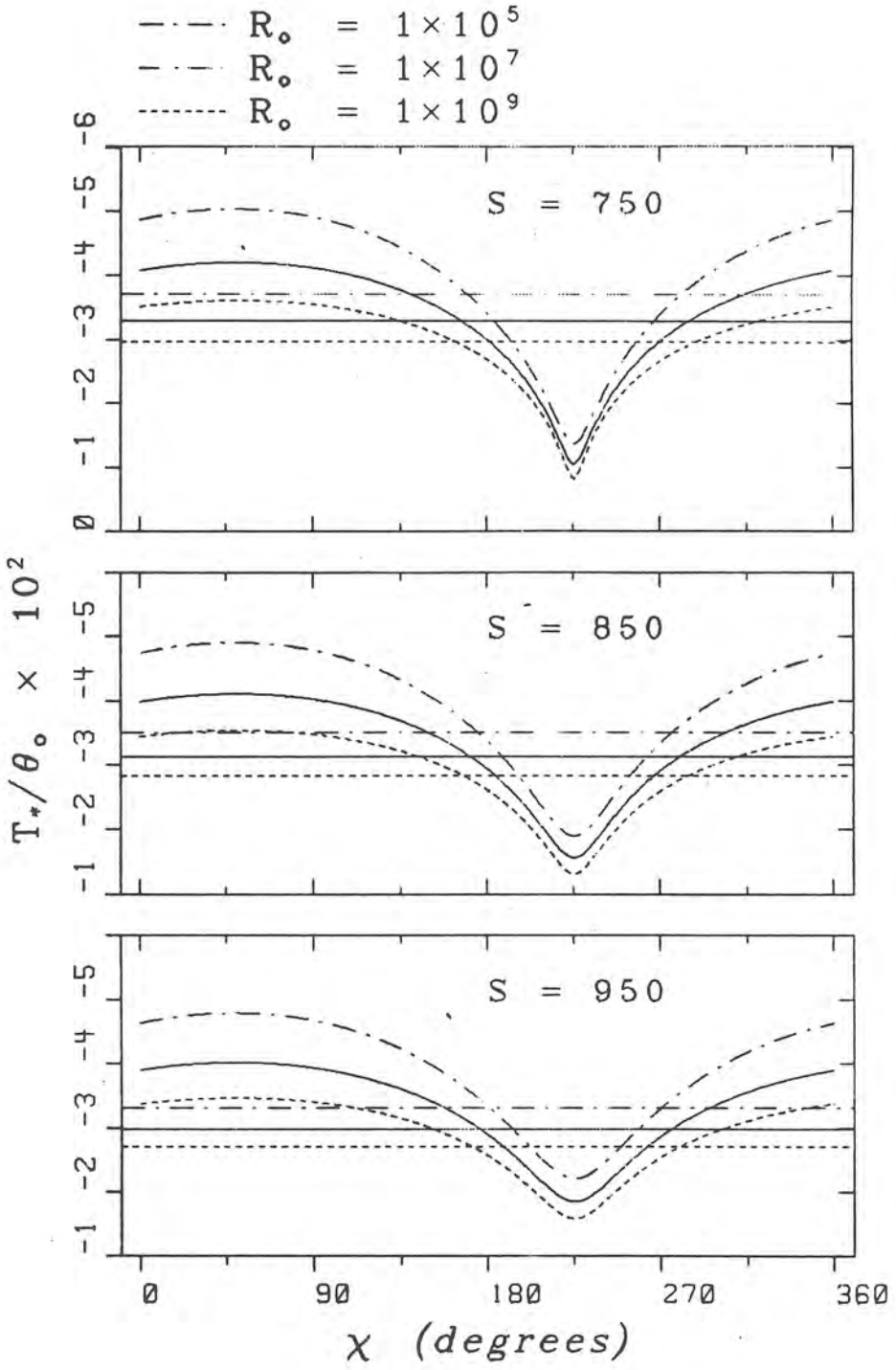

FIGURE 13. The same as Figure 10 except for the 'staircase' regime.

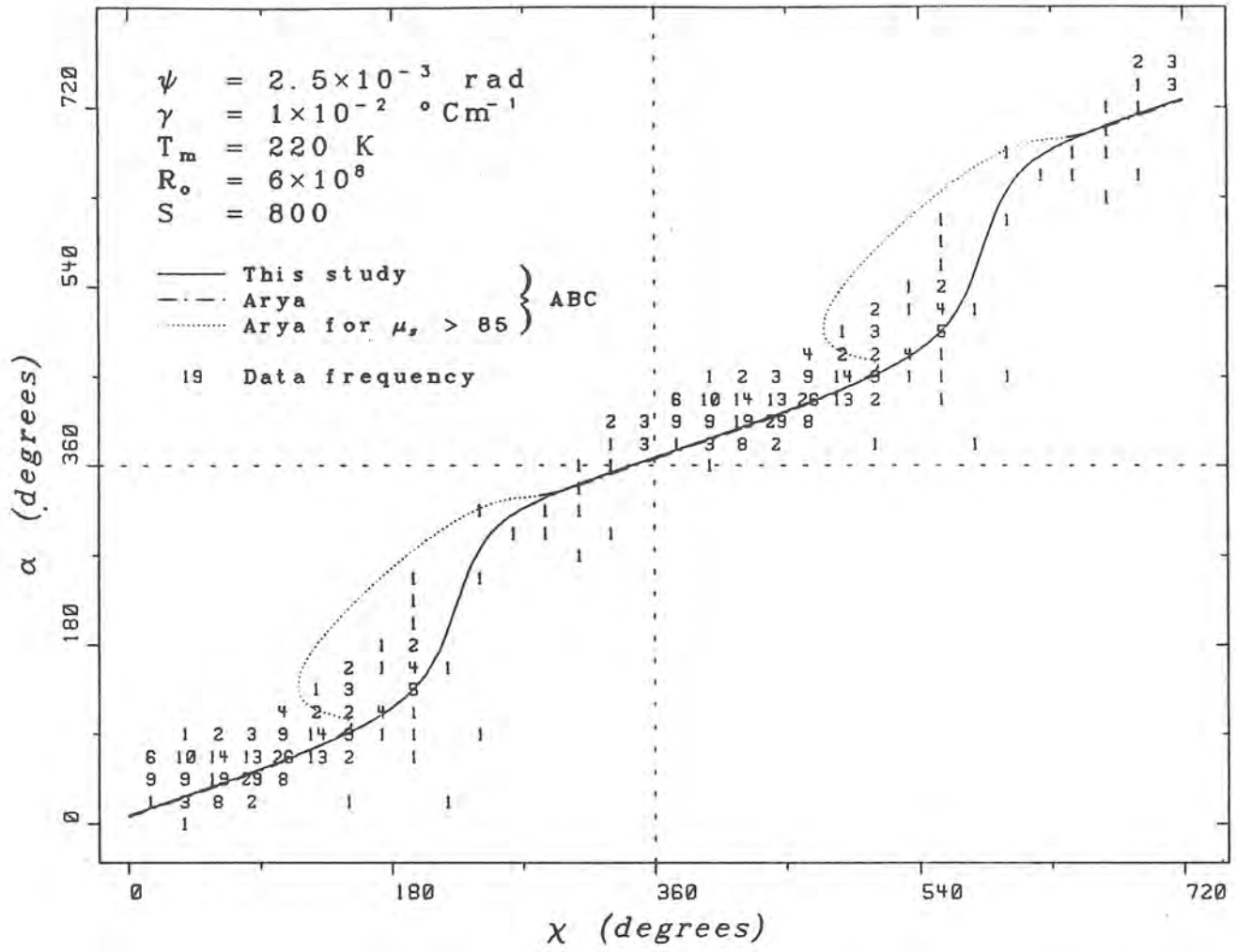

FIGURE 14. A comparison of observed angle α at the South Pole with the results of this investigations as a function of χ. The values of the other parameters are as indicated in the figure. The numbers inside the diagram indicate the frequency of occurence of the observed values. The solid curve is for the A, B and C functions of this investigation and the dot-dashed curve for Araya's functions. The dotted portion of the dot-dashed curve between 152.15 < χ 281.13 deg is the interval where Araya's functions cease to be useful. Note that in order to make the comparison possible at <u>any</u> interval in χ the curves are plotted over two cycles.

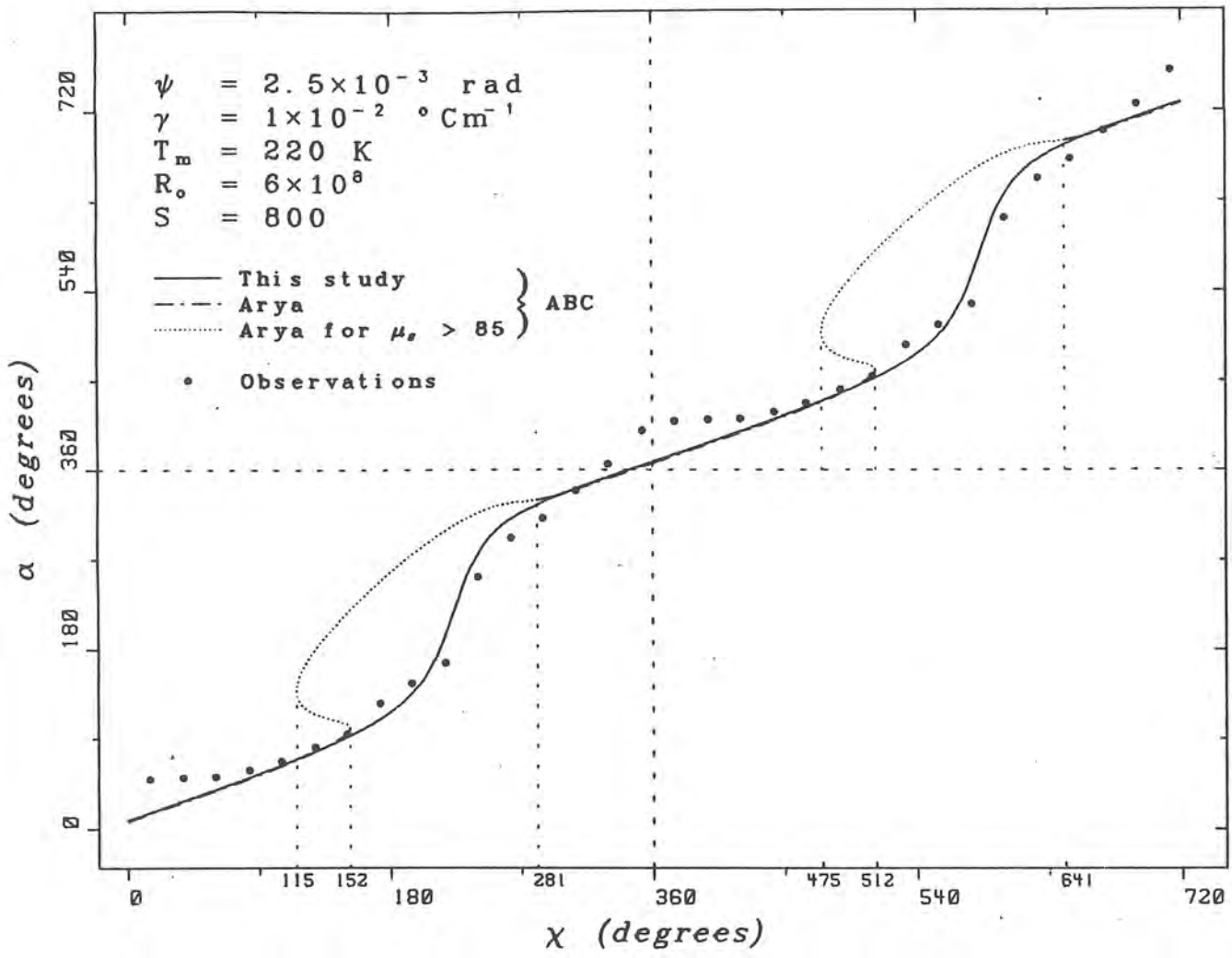

FIGURE 15. The same as Figure 14, except that the data points denoted by dots are the '3-column running' means of the observed values in Table II or Figure 14. The dot-dashed curve shows that: (1) α is continuous in the intervals $0 \leq \chi \leq 152.15$ and $\chi > 281.13$ deg; (2) α is discontinuous at $\chi = 152.15$ deg; (3) α has multiple solutions in the interval $115.42 < \chi < 152.15$ deg.

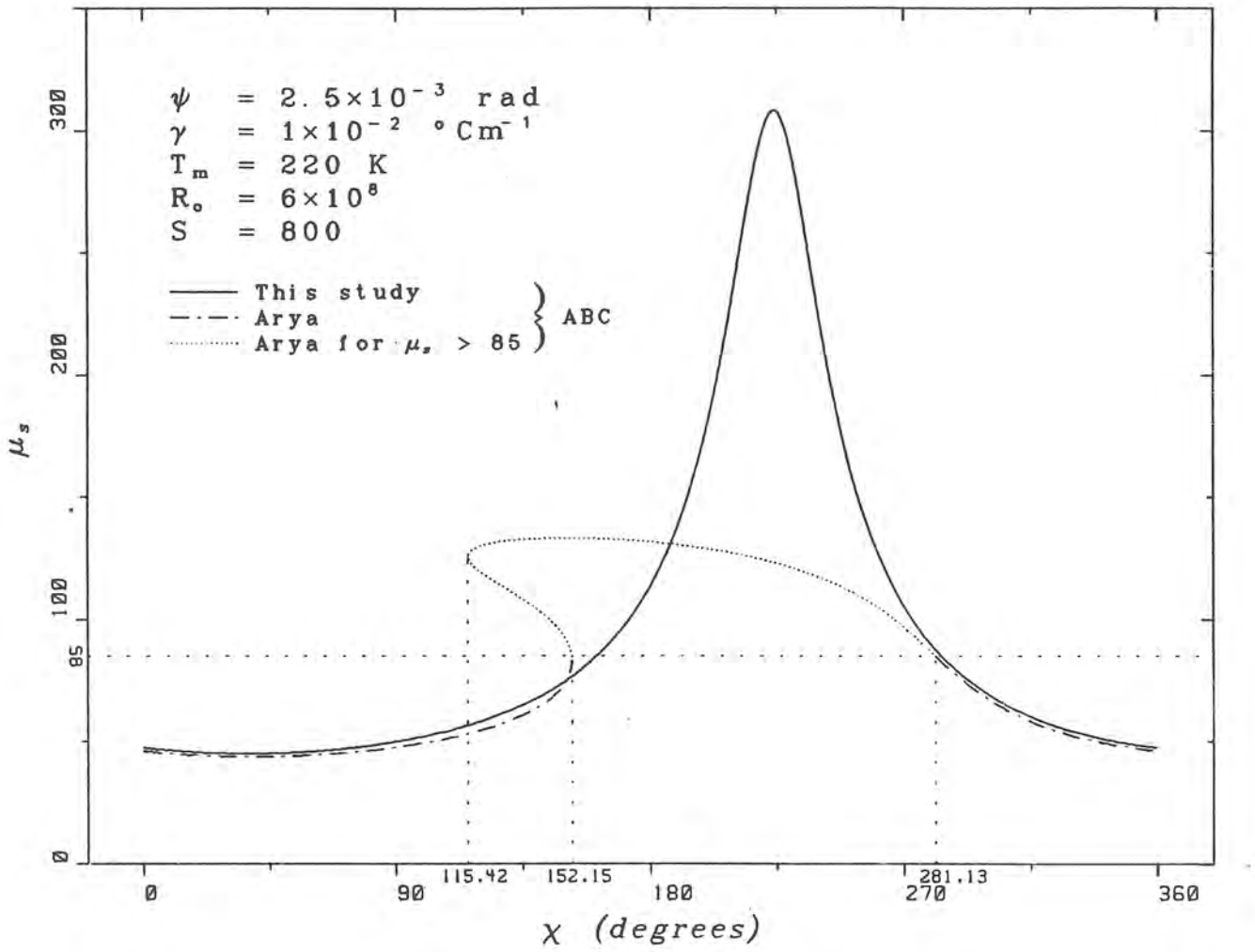

FIGURE 16. Solutions of μ_s versus χ for the same parameters as in Figures 14 and 15. The dot-dashed curve shows that: (1) $\mu_s \leq 82.76$ and $\mu_s < 85.00$ in the intervals $0 \leq \chi < 152.15$ and $\chi > 281.13$ deg respectively; (2) $\mu_s > 85$ in the interval $152.15 < \chi < 281.13$ deg (where Araya's A, B and C functions are no longer useful) and μ_s is discontinuous at $\chi = 152.15$ deg; (3) $85 < \mu_s < 85$ in the interval $115.42 < \chi < 152.15$ deg. There are no observations of μ_s for comparison.

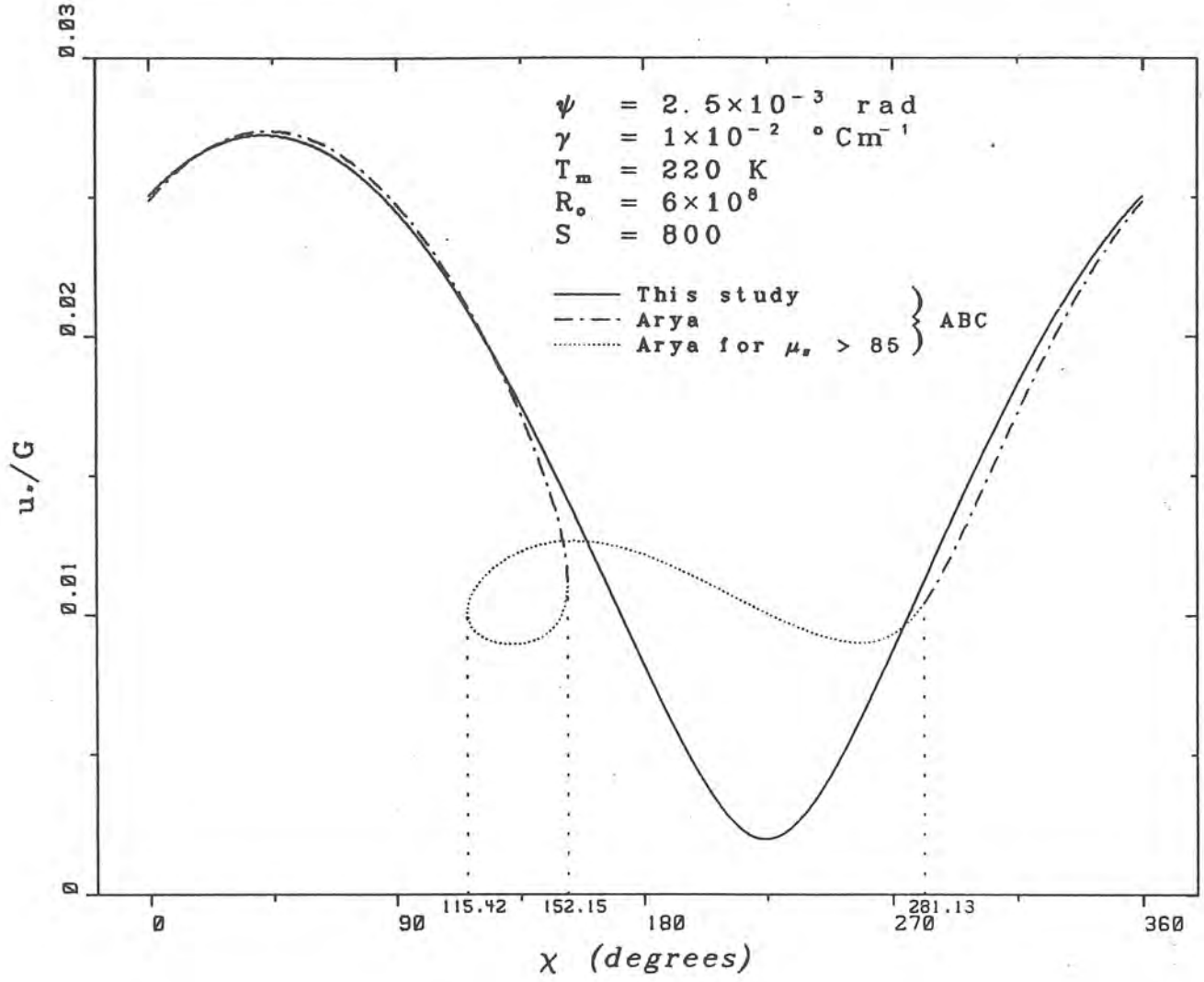

FIGURE 17. The same as Figure 16, except for u_*/G. However, in this case there is no discontinuity at χ = 152.15 deg.

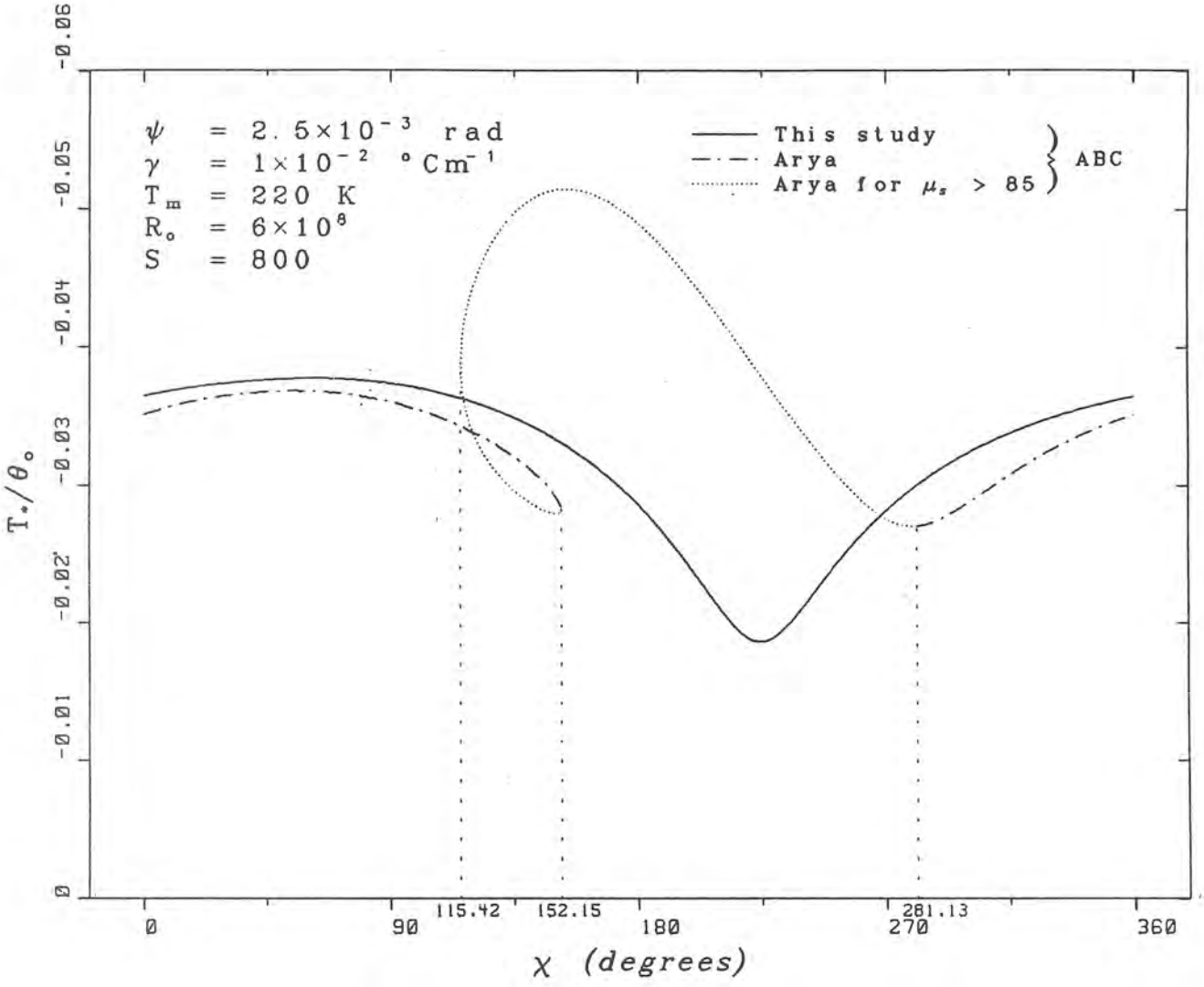

FIGURE 18. The same as Figure 16, except for T_*/Θ_0; as was the case with α and μ_s it has a discontinuity at χ 152.15 deg.

SMHI Rapporter, METEOROLOGI OCH KLIMATOLOGI (RMK)

Nr 1 Thompson, T, Udin, I, and Omstedt, A
Sea surface temperatures in waters surrounding Sweden
Stockholm 1974

Nr 2 Bodin, S
Development on an unsteady atmospheric boundary layer model.
Stockholm 1974

Nr 3 Moen, L
A multi-level quasi-geostrophic model for short range weather predictions
Norrköping 1975

Nr 4 Holmström, I
Optimization of atmospheric models
Norrköping 1976

Nr 5 Collins, W G
A parameterization model for calculation of vertical fluxes of momentum due to terrain induced gravity waves
Norrköping 1976

Nr 6 Nyberg, A
On transport of sulphur over the North Atlantic
Norrköping 1976

Nr 7 Lundqvist, J-E, and Udin, I
Ice accretion on ships with special emphasis on Baltic conditions
Norrköping 1977

Nr 8 Eriksson, B
Den dagliga och årliga variationen av temperatur, fuktighet och vindhastighet vid några orter i Sverige
Norrköping 1977

Nr 9 Holmström, I, and Stokes, J
Statistical forecasting of sea level changes in the Baltic
Norrköping 1978

Nr 10 Omstedt, A, and Sahlberg, J
Some results from a joint Swedish-Finnish sea ice experiment, March, 1977
Norrköping 1978

Nr 11 Haag, T
Byggnadsindustrins väderberoende, seminarieuppsats i företagsekonomi, B-nivå
Norrköping 1978

Nr 12 Eriksson, B
Vegetationsperioden i Sverige beräknad från temperaturobservationer
Norrköping 1978

Nr 13 Bodin, S
En numerisk prognosmodell för det atmosfäriska gränsskiktet grundad på den turbulenta energiekvationen
Norrköping 1979

Nr 14 Eriksson, B
Temperaturfluktuationer under senaste 100 åren
Norrköping 1979

Nr 15 Udin, I, och Mattisson, I
Havsis- och snöinformation ur datorbearbetade satellitdata - en modellstudie
Norrköping 1979

Nr 16 Eriksson, B
Statistisk analys av nederbördsdata. Del I. Arealnederbörd
Norrköping 1979

Nr 17 Eriksson, B
Statistisk analys av nederbördsdata. Del II. Frekvensanalys av månadsnederbörd
Norrköping 1980

Nr 18 Eriksson, B
Årsmedelvärden (1931-60) av nederbörd, avdunstning och avrinning
Norrköping 1980

Nr 19 Omstedt, A
A sensitivity analysis of steady, free floating ice
Norrköping 1980

Nr 20 Persson, C och Omstedt, G
En modell för beräkning av luftföroreningars spridning och deposition på mesoskala
Norrköping 1980

Nr 21 Jansson, D
Studier av temperaturinversioner och vertikal vindskjuvning vid Sundsvall-Härnösands flygplats
Norrköping 1980

Nr 22 Sahlberg, J and Törnevik, H
A study of large scale cooling in the Bay of Bothnia
Norrköping 1980

Nr 23 Ericson, K and Hårsmar, P-O
Boundary layer measurements at Klockrike. Oct. 1977
Norrköping 1980

Nr 24 Bringfelt, B
A comparison of forest evapotranspiration determined by some independent methods
Norrköping 1980

Nr 25 Bodin, S and Fredriksson, U
Uncertainty in wind forecasting for wind power networks
Norrköping 1980

Nr 26 Eriksson, B
Graddagsstatistik för Sverige
Norrköping 1980

Nr 27 Eriksson, B
Statistisk analys av nederbördsdata. Del III. 200-åriga nederbördsserier
Norrköping 1981

Nr 28 Eriksson, B
Den "potentiella" evapotranspirationen i Sverige
Norrköping 1981

Nr 29 Pershagen, H
Maximisnödjup i Sverige (perioden 1905-70)
Norrköping 1981

Nr 30 Lönnqvist, O
Nederbördsstatistik med praktiska tillämpningar
(Precipitation statistics with practical applications)
Norrköping 1981

Nr 31 Melgarejo, J W
Similarity theory and resistance laws for the atmospheric boundary layer
Norrköping 1981

Nr 32 Liljas, E
Analys av moln och nederbörd genom automatisk klassning av AVHRR data
Norrköping 1981

Nr 33 Ericson, K
Atmospheric Boundary layer Field Experiment in Sweden 1980, GOTEX II, part I
Norrköping 1982

Nr 34 Schoeffler, P
Dissipation, dispersion and stability of numerical schemes for advection and diffusion
Norrköping 1982

Nr 35 Undén, P
The Swedish Limited Area Model (LAM). Part A. Formulation
Norrköping 1982

Nr 36 Bringfelt, B
A forest evapotranspiration model using synoptic data
Norrköping 1982

Nr 37 Omstedt, G
Spridning av luftförorening från skorsten i konvektiva gränsskikt
Norrköping 1982

Nr 38 Törnevik, H
An aerobiological model for operational forecasts of pollen concentration in th air
Norrköping 1982

Nr 39 Eriksson, B
Data rörande Sveriges temperaturklimat
Norrköping 1982

Nr 40 Omstedt, G
An operational air pollution model using routine meteorological data
Norrköping 1984

Nr 41 Christer Persson and Lennart Funkquist
Local scale plume model for nitrogen oxides.
Model description.
Norrköping 1984

Nr 42 Stefan Gollvik
Estimation of orographic precipitation by dynamical interpretation of synoptic model data.
Norrköping 1984

Nr 43 Olov Lönnqvist
Congression - A fast regression technique with a great number of functions of all predictors.
Norrköping 1984

Nr 44 Sten Laurin
Population exposure to $So_2$and NO_x from different sources in Stockholm.
Norrköping 1984

Nr 45 Jan Svensson
Remote sensing of atmospheric temperature profiles by TIROS Operational Vertical Sounder.
Norrköping 1985

Nr 46 Bertil Eriksson
Nederbörds- och humiditetsklimat i Sverige under vegetationsperioden
Norrköping 1986

Nr 47 Roger Taesler
Köldperioder av olika längd och förekomst
Norrköping 1986

Nr 48 Wu Zengmao
Numerical study of lake-land breeze over Lake Vättern Sweden
Norrköping 1986

Nr 49 Wu Zengmao
Numerical analysis of initialization procedure in a two-dimensional lake breeze model
Norrköping 1986

Nr 50 Persson, Christer
Local scale plume model for nitrogen oxides. Verification.
Norrköping 1986

Nr 51 Melgarejo, José W.
An analytical model of the boundary layer above sloping terrain with an application to observations in Antarctica
Norrköping 1986

SMHI
Swedish meteorological and hydrological institute
S-60176 Norrköping, Sweden. Tel. +4611158000. Telex 64400 smhi s.

ISSN 0347-2116